Lesson 1

1.1 Introduction

This course deals with the problems of nucleation, spinodal decomposition and continuous ordering and domain growth. The first and most obvious question we will address is what are these processes. Answering this question will occupy us for the next two weeks.

We will begin by looking at the phenomology and taking a broad brush look at the experimental data, both numerical and "real". The easiest way to start is by considering the van der Waals equation for a simple one component fluid. Figure 1 contains a sketch of the pressure p vs. the density ρ for $T < T_c$, where T_c is the critical temperature.

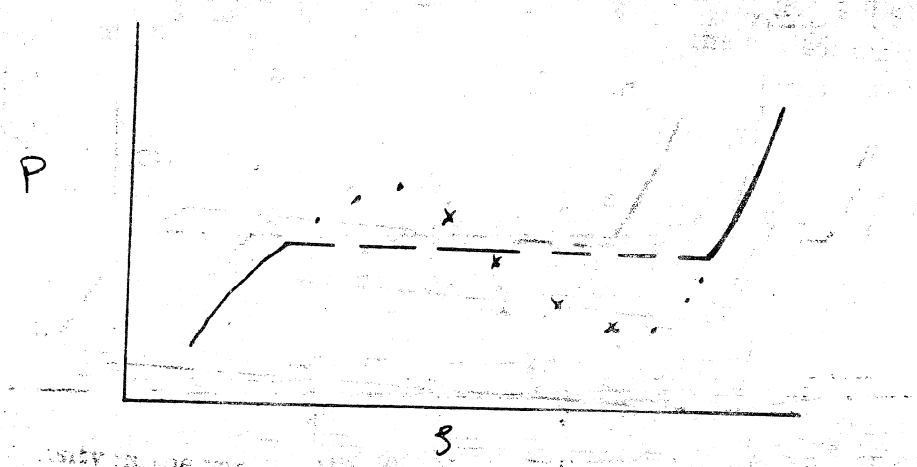

Fig. 1 Pressure vs. density in the van der Waals theory for $T < T_c$. The dashed line is the Maxwell construction, the dotted lines metastable states and the crosses unstable states.

The solid lines represent the equilibrium gas (small ρ) and liquid (large ρ) phases. The dashed line represents the Maxwell construction, the region of coexistence between liquid and gas, which is also in equilibrium. Our investigations concern the region represented by the dotted line and the line of crosses.

The line of crosses represents a region of instability. On this line the isothermal compressibility $\kappa_T \sim [\partial p/\partial \rho]_T^{-1} < 0$ which implies that increasing the pressure lowers the density. This clearly nonsensical result occurrs because we are trying to describe the system in a region of rapid time development with an equilibrium theory.

The dotted lines represent metastable states. Here there is no obvious contradiction generated by the use of equilibrium methods. To understand the metastable state we will use a slightly different thermodynamic point of view. Remembering that[1] the chemical potential μ is the Gibbs free energy per particle and that

$$\mu = \int^p v(p')dp' + \phi(T) \tag{1.1}$$

where $v(p) = \rho^{-1}$ and $\phi(T)$ is an undetermined function of the temperature, we use the van der Waals equation to obtain $v(p)$ and obtain the free energy vs. pressure curve drawn schematically in fig. 2.

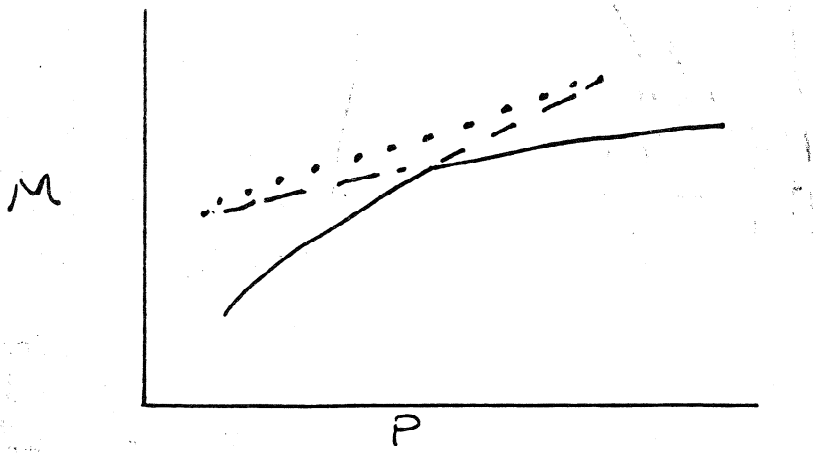

Fig. 2 The free energy as a function of pressure. The solid lines represent stable states, the dashed lines metastable and the dotted line unstable states.

Note first that the dotted line which is obtained from integration of the negative κ_T region of fig. 1. is concave, indicating again that this region is unstable. The rest of the curve is convex. That is, in the metastable and stable regions the Gibbs free energy is a convex function of the pressure indicating a positive response function or compressibility. However the part of the curve represented by the dashed line lies **above** the solid line. Hence the region we have labeled metastable has a higher free energy than the stable phase. Moreover, thermodynamic states (metastable state, unstable and even unstable) are associated with free enery extrema, which implies that the metastable state is a local rather than a global minimum of the free energy. We will return to this point shortly.

Returning to fig. 1 note the two points where the dotted lines and lines of crosses meet. At these points $\kappa_T \to \infty$ These are the spinodal points which we will discuss in some detail in later lectures. Here we simply note that spinodals are critical points with not only a divergent compressibility but which have many of the same features of usual critical points.

In fig. 3 we have plotted the locus of the spinodal points (dashed line) and the end points of the Maxwell construction (solid line) as the temperature is varied. These lines are the spinodal curve, which separates the metastable region from the unstable in the mean-field picture, and the coexistence curve.

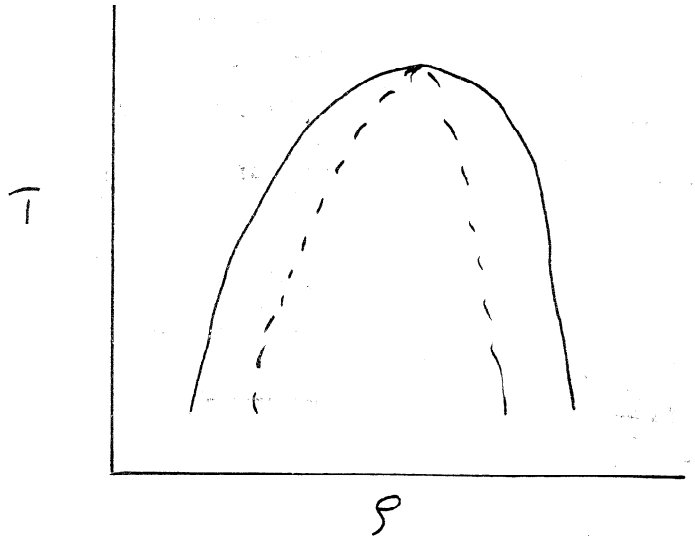

Fig. 3 Coexistence and spinodal curves.

Neither the unstable or metastable state corresponds to an absolute minimum of the free energy and hence they cannot last forever; that is a property of equilibrium. Consequently, if we prepare a system in one of these states some decay process must occur which eventually brings the system into equilibrium.

In our considerations so far we have been using the liquid-gas transition as a model but our considerations are quite general. If, for example we wanted to describe the phase separation of a binary mixture of two different molecules A and B, the same diagrams can be used with a relabeling of the axes. In fig. 3 for example the x axis rather than being the density is the difference in concentration of the two components, $\Delta\rho_{AB}$. The only difference in the two digrams is the so called order parameter.

The order parameter is the variable that specifies the structure of the phase transition. It is non-zero in the ordered phase and if it is discontinuous at the phase transition then the transition is first order. If the order parameter **derivative** is discontinuous at the transition then the transition is second order (e. g. critical points).

Our next step is to look at some pictures of these decay processes. In fig. 4 we have reproduced[2] pictures obtained from a transmission electron microscope study of an iron aluminum alloy undergoing phase separation. The outer two columns illustrate the temporal evolution (from top to bottom) subsequent to a quench to two different points in the metastable region. The middle column is the result of a quench into an unstable state. The outer columns are characterized by the appearence some time after the quench of isolated droplets which then grow. The quench into the unstable region is

followed by the appearence of an interconnected structure. These interconnected structures grow and coarsen. For late times, evolution from both the metastable and

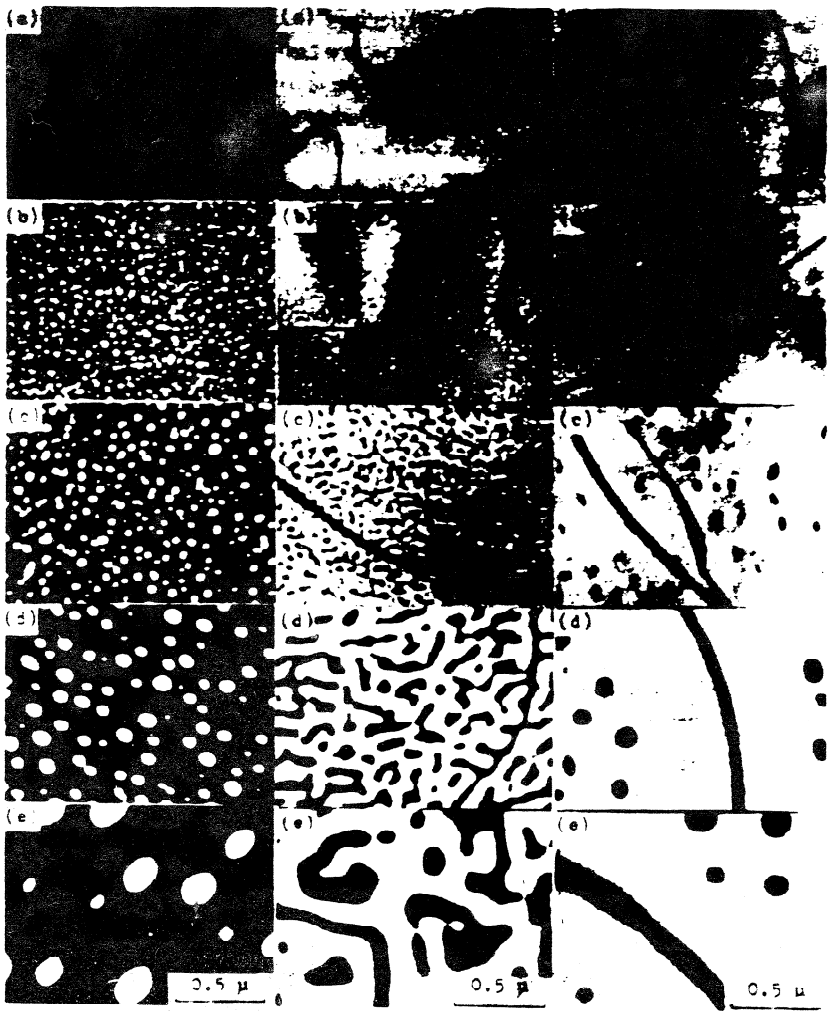

FIG. 3. Domain structures imaged with B_2 superlattice reflection in 23.0, 24.7 and 24.9 at% Al alloys, from left to right. The samples are quenched from 630°C and annealed at 570°C in the case of 23.0 and 24.7 at% Al alloys and at 568°C in the case of 24.9 at% Al alloy. (a) As quenched; (b) annealed for 15 min in 23.0 and 24.9 at% Al and for 10 min in 24.7 at% Al alloy; (c) 100 min; (d) 1000 min; (e) 10000 min. (From Oki *et al.*, 197[illegible])

Fig. 4 Temporal evolution of an Iron-Aluminum alloy quenched into the metastable (outer columns) and unstable (center column) regions.

unstable region evolves into the growth of large isolated droplets. In this state the system has lost all memory of the initial quench.

At this point we can define the processes we will be studying this semester. Nucleation is the mechanism by which the metastable state decays and is characterized by the appearence sometime after the quench of isolated regions or droplets that grow and become the stable phase. Late stage domain growth is concerned with the way these droplets or regions (we will also refer to them as clusters) grow in the very late stages of their evolution.

Finally spinodal decomposition is the mechanism by which the unstable state begins to decay if the **order paramter is conserved** and continuous ordering is the same process when the order parameter is **not conserved.**

In the next three sections we will construct simple theories to describe these three processes. Although these theories are crude they get a lot of the physics right and will be our starting points for more sophisticated approaches to follow.

1.2 Nucleation - Simple Theory

As we saw earlier there does not appear to be any contradictions when we treat the metastable state with equilibrium methods. The metastable state however is not characterized as the absolute or global minimum of the free energy. In order to obtain more insight into the properties of this state and to develop a foundation for more sophisticated theoretical approaches we will look at one more approach to this problem, the so called Landau - Ginzburg theory. First however, we will slightly broaden the class of models we will consider. It will be easier to make contact with the numerical or simulation work if we consider the Ising model.

Consider a lattice with a spin at each vertex (fig. 5). These spins can be in one of two directions, up or down. The variable that describes the spins we will call s_i where i labels the vertex and $s_i = \pm 1$. The Hamiltonian is given by

$$-\beta H = \sum_{ij} K(ij) s_i s_j - h \sum_i s_i \tag{1.2}$$

where $\beta = [k_B T]^{-1}$ and h is an applied uniform field. Note that there is an absorbed minus sign. The first sum is over pairs of spins but they need not be nearest neighbors. In this course we will always assume $K(ij) > 0, \forall i, j$

This model (the Ising model) has been studied extensively and we will return to it often. For now we simply note that the identification of, for example, a down spin with an

occupied site and an up spin with an empty one gives us a simple model for the liquid-gas transition. In a similar manner, identification of an up spin with an A atom and a down spin with a B gives us a model for a binary system. The Ising model itself is a model for a uniaxial magnet.

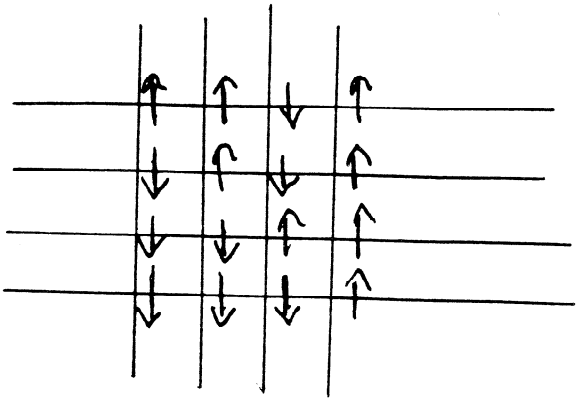

Fig. 5 Square lattice in two dimensions with an Ising spin at each vertex

Figure 6 is a schematic plot of the magnetization as a function of the magnetic field for $T < T_c$ for the mean-field version of the Ising model. Figure 7 is the corresponding coexistence curve and spinodal.

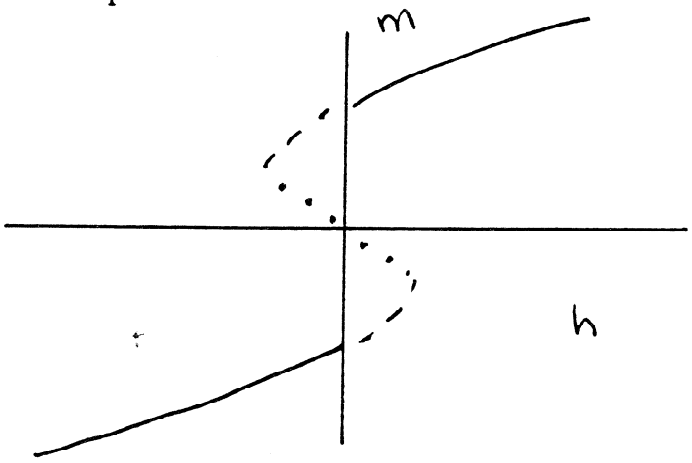

Fig. 6 Magnetization as a function of magnetic field for $T < T_c$

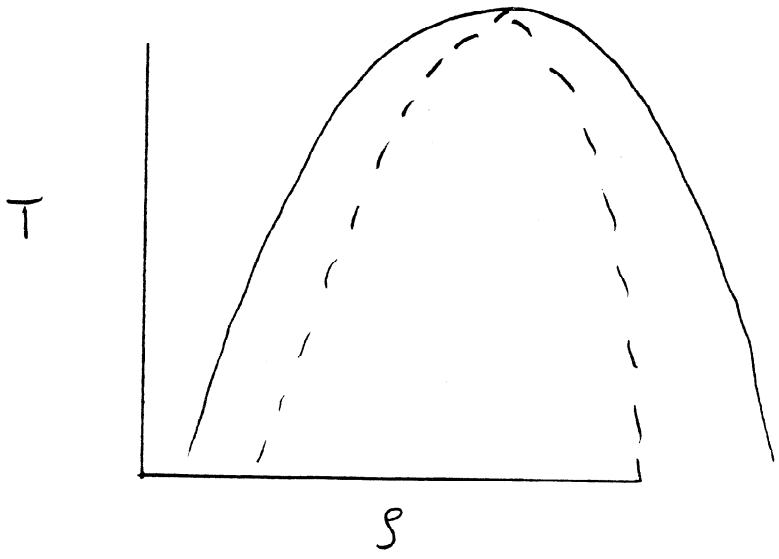

Fig. 7 Coexistence curve and spinodal. The density $\rho = (1 + m)/2$

Although this model is relatively simple and a great deal is known about its equilibrium properties it is still difficult to manage in the metastable and unstable regions. We will look at an even simpler model obtained from the Ising model by the process of coarse graining.

The idea is to take the lattice in fig. 5 and block it off into squares L on a side. We will refer to L as the coarse graining size. We can now define a local coarse grained order parameter, $\psi(\vec{x})$, which is the sum of the local microscopic variables over the box centered at $\vec{x}$. The quantity $\psi(\vec{x})$ will now be our fundemental unit rather than the s_i. In the Ising model for example we define $\psi(\vec{x})$ through the equation

$$\psi(\vec{x}) = L^{-d} \sum_{i \epsilon L(\vec{x})} s_i \tag{1.3}$$

where $L(\vec{x})$ is a box of size L centered at $\vec{x}$. Our aim is to develop a description of the phenomena of interest in terms of the $\psi(\vec{x})$. If this is to make any sense then we must require that $L >> a$ where a is the fundemental microscopic length in the problem. In the Ising model a would be the lattice constant. We must also have that $L << \ell$ the dominant statistical length in the problem. We require the latter so that the physics of interest is not washed away in the coarse graining proceedure and we require the former so that the fluctuations of the $\psi(\vec{x})$, which we will ignore, are small.

It is important to understand that ℓ need not be the correlation length. For example in nucleation ℓ would be the size of the critical droplet which can be significantly larger than the correlation length.

We now postulate what might be called a phenomenological free energy $F(\psi)$. Again using the Ising model as our paradigm we will consider the Helmholz free energy of a

system in contact with a heat bath.[1]

$$F(\psi) = -h\int \psi(\vec{x})d\vec{x} - \frac{1}{2}\int\int K(|\vec{x}-\vec{y}|)\psi(\vec{x})\psi(\vec{y})d\vec{x}d\vec{y} \\ - K_BT\int[1+\psi(\vec{x})]\ln(1+\psi(\vec{x}))d\vec{x} + K_BT\int[1-\psi(\vec{x})]\ln(1-\psi(\vec{x}))d\vec{x} \tag{1.4}$$

The first term is the interaction of the coarse grained $\psi(\vec{x})$ with an external magnetic field. The second term is the interaction between coarse grained blocks which we have assumed to be dependent only on the distance between blocks. The last two terms are the entropy which can be obtained by considering the (natural) log of the number of states and using Stirlings approximation. Note that the up - down symmetry for $h = 0$ of the Ising model is preserved. (Also see ref. 2 for additional discussion.)

This model free energy is certainly simpler than the Ising model free energy obtained from the log of the partition function but we will simplify it yet again by making two assumptions. First we will assume that $\psi(\vec{x})$ is small so that the logrithms can be expanded and the expansion truncated after the quardic term. Our second assumption can be best seen by going into Fourier space using Parseval's theorem and writing the interaction between blocks as

$$\frac{1}{2}\int \hat{K}(|\vec{k}|)\hat{\psi}(\vec{k})\psi(\vec{k})d\vec{k} \tag{1.5}$$

Expanding $\hat{K}(|\vec{k}|)$ in a power series in $k = |\vec{k}|$ and keeping only up to quadratic terms we obtain upon returning to $\vec{x}$ space

$$\hat{K}(0)\int \psi(\vec{x})\psi(\vec{x})d\vec{x} + \frac{1}{2}R^2\int[\nabla\psi(\vec{x})]^2d\vec{x} \tag{1.6}$$

where $R^2 \propto \int x^2K(x)d\vec{x}$, $x = |\vec{x}|$, and integration by parts has been used. The truncation of the power series in k is an assumption that the $\psi(\vec{x})$ are slowly varying so that significant changes can only occurr over large distances.

With these assumptions our model becomes

$$F(\psi) = \int d\vec{x}\{R^2[\nabla\psi(\vec{x})]^2 + \epsilon\psi^2(\vec{x}) + \psi^4(\vec{x}) - h\psi(\vec{x})\} \tag{1.7}$$

with

$$\epsilon = K_BT - \hat{K}(0) \tag{1.8}$$

This is the Landau-Ginsburg free energy which can be obtained in several ways. Useful descriptions can be found in refs. 2-4. Note that our original interaction was positive so that the interaction between blocks is also positive. This implies that $\hat{K}(0) > 0$. Also note

that this Landau-Ginsburg form, with small changes is also applicable to the other models we discussed.

One more point about eqs. 1.4 and 1.7. This model is clearly mean-field. The reason of course is that the free energy, unlike the Hamiltonian is a thermodynamic quantity. This makes it necessary to interpret $\psi(\vec{x})$ as an average quantity, ie. averaged over time or ensembles. Our definition of $\psi(\vec{x})$ in eq. 1.3 does not take either of these averages. Consequently the only way we can make a thermodynamic free energy consistent with an unaveraged $\psi(\vec{x})$ is to assume that only one configuration is important and hence averaging is unnecessary. This means ignoring fluctuations which implies mean-field. One should expect therefore that the Landau - Ginsburg free energy will produce results consistent with mean-field theory.

We now return to consideration of the metastable state in the mean-field approximation. As some of you may know the van der Waals equation without the Maxwell construction is "derived" with the condition of spatial uniformity. This condition is what gives rise to the van der Waals loop. With the same assumption the free energy in eq. 1.7 becomes

$$f(\psi) = \frac{F(\psi)}{V} = \epsilon\psi^2 + \psi^4 - h\psi \tag{1.9}$$

where V is the volume of the system.

From eq. 1.8 it is clear that for high temperatures $\epsilon > 0$ The free energy per unit volume (or per spin) has the form shown in fig. 8.

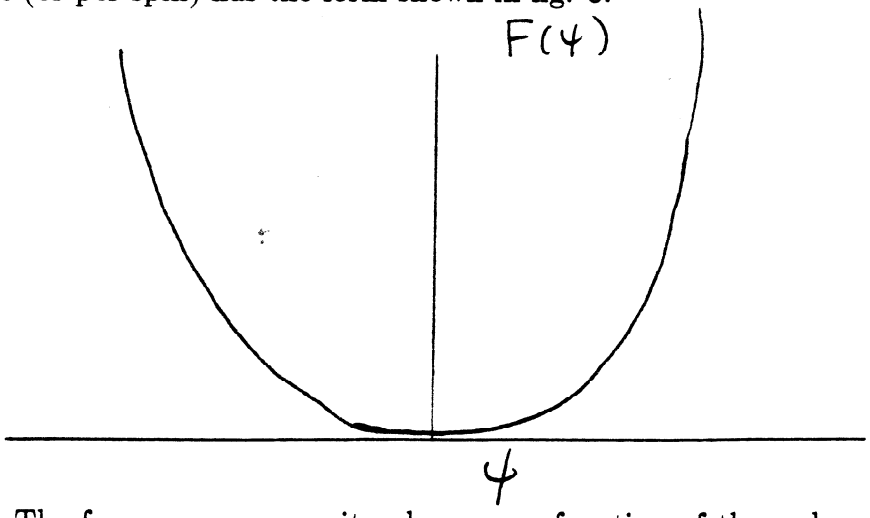

Fig. 8 The free energy per unit volume as a function of the order parameter for high T and $h = 0$.

There is one minimum at $\psi = 0$. As T is lowered the the critical temperature T_c is reached where $\epsilon = 0$. If $h = 0$ this is the critical point. It is a simple matter to obtain the static critical exponents for this model[6] which are mean-field as expected.

If T is lowered below T_c then the $f(\psi)$ develops three extrema, 2 minima and a maximum.(fig. 9)

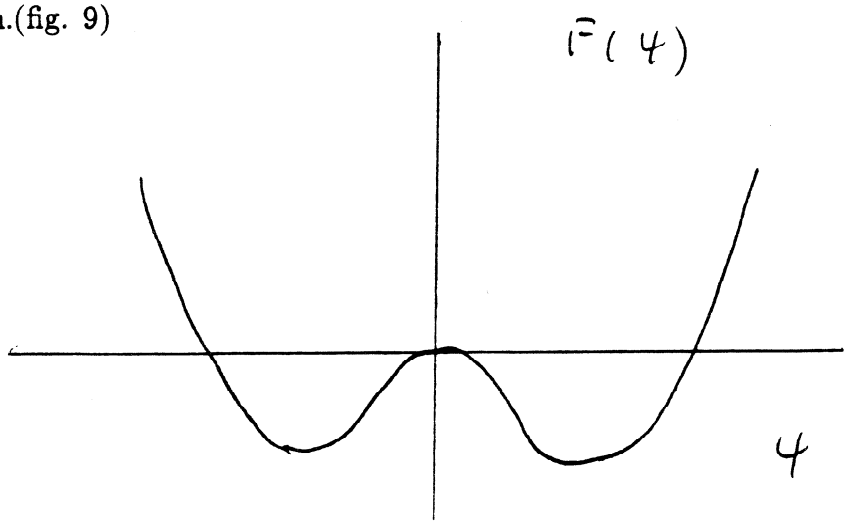

Fig. 9a Free energy per unit volume vs order parameter for $\epsilon < 0$ and $h = 0$

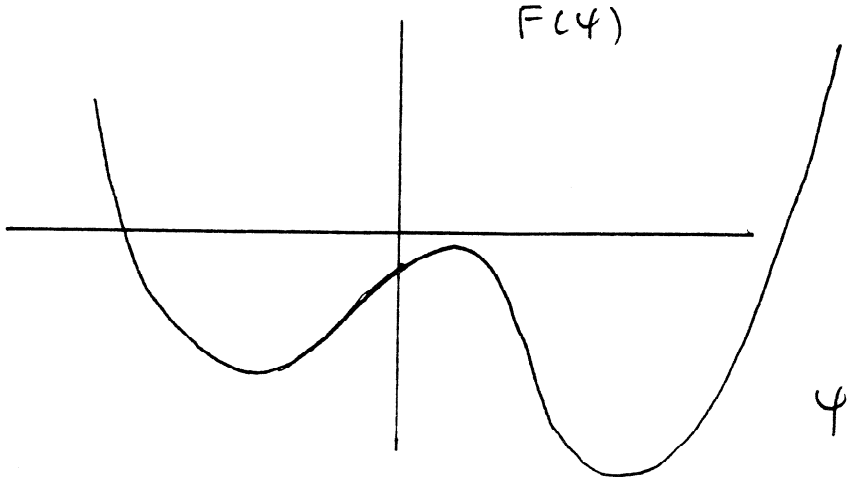

Fig. 9b Free energy per unit volume for $\epsilon < 0$ and $h > 0$

To make contact with fig. 2 think of fixing the temperature and generating a change in the pressure p. You will move along the curve $\mu(p)$ in fig. 2. The same change in pressure will generate, in the language of fig. 9, a change in the shape of the free energy vs ψ curve. The absolute minimum will track the stable part of the curve in fig. 2, the relative minimum the metastable branch and the maximum the unstable branch. When the relative minimum and the maximum come together in fig. 9 the spinodal is reached in fig. 2.

The metastable state then is a relative minimum of the free energy. It will act like a thermodynamically stable state until a fluctuation probes the thermodynamic space far enough away from the local minimum that the system "knows" there is a lower free energy elsewhere. At this point the decay of the metastable state begins. We now make a rather

strong assumption; The fluctuations that initiate the decay of the metastable state can be treated as equilibrium fluctuations about the metastable local minimum of the free energy. This assumption can only hold if the metastable state lasts long enough that metastable equilibrium is attained. How long is that? No one knows. It is a point we will return to.

Let us live with this assumption for a while and see where it leads us. We know experimentally that the metastable state last a long time if we are close to the coexistence curve. In this region we can also see that the number of droplets that appear and grow in some time interval is small and the droplets are isolated, i. e. non - interacting. Near the coexistence curve the droplets also appear to be compact, that is not stringy or seaweed like. They also appear large enough to treat with macroscopic ideas such as free energy and surface tension. These observations lead to the following assumptions.

- Nucleation is initiated by isolated, non - interacting droplets which can be treated as fluctuations about metastable equilibrium.
- The droplets are compact with a surface and interior that can be considered separately.
- The interior and surface free energy density are well defined.
- The surface free energy density (surface tension) is relatively insensitive to quench depth.
- The interior free energy density is equal to the free energy density of the **stable phase**

These are the assumptions that go into the so called classical theory of nucleation. We can determine the free energy cost ΔF to produce one of these critical or nucleating droplets. From the assumptions above it will have two contributions; a surface term that raises the free energy (since it costs free energy to have a boundary between two different phases) and a bulk term that lowers it.

$$\Delta F = -|\Delta f| r^d + \sigma r^{d-1} \tag{1.10}$$

where σ is the surface tension, Δf the interior free energy density difference between the metastable state and the droplet interior (assumed negative), r the droplet radius and d the dimension of space.

From the plot of ΔF vs r in fig. 10 we can see that systems get trapped in meta - stable states because small fluctuations tend to decay rather than grow because decaying lowers the free energy. Big enough fluctuations on the other hand tend to grow because growing lowers the free energy. The critical droplet is the one for which growth and decay are equally likely. From fig. 10 that is clearly the droplet with a radius corresponding to the maximum of the ΔF curve.

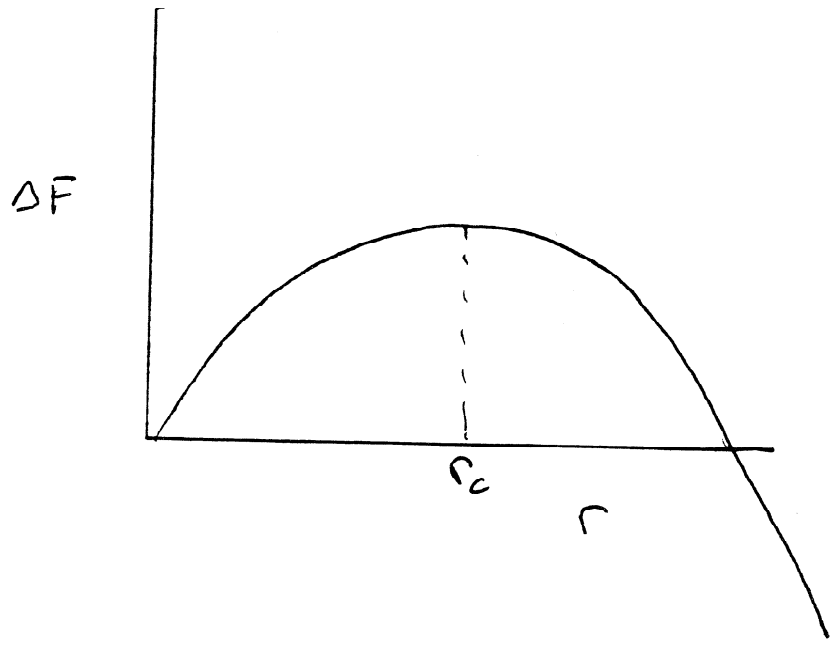

Fig. 10

The critical radius r_c, ie the radius of the critical droplet, is obtained by differentiating ΔF and setting the derivative equal to zero. From eq. 1.10 we have

$$r_c \propto \frac{\sigma}{\Delta f} \tag{1.11}$$

and

$$\Delta F_c \propto \frac{\sigma^d}{\Delta f^{d-1}} \tag{1.12}$$

where ΔF_c is the free energy cost of a critical droplet.

Since the droplets are non - interacting equilibrium fluctuations, the probability of finding a critical droplet is inversely proportional to the time τ spent in the metastable state before one appears. This is roughly the lifetime of the metastable state.

$$\tau \propto \exp[\frac{\Delta F_c}{K_B T}] \tag{1.13}$$

If the quench into the metastable state terminates near the coexistence curve then $\Delta f << 1$ and the lifetime of the metastable state is large. We assumed that the system would settle into metastable equilibrium before the critical droplet initiated the decay and for large τ this would seem reasonable. Suppose however the quench takes the system far from the coexistence curve. From fig. 9 we see that the free energy difference Δf increases and hence ΔF_c decreases. For many systems ΔF_c can become the order of a few $K_B T$. For these systems undergoing deep quenches the metastable state cannot be maintained long enough for the assumption of metastable equilibrium to be valid. The quench depth at which this takes place is often called the limit of metastability or sometimes the Becker-Döring limit.(fig. 11)

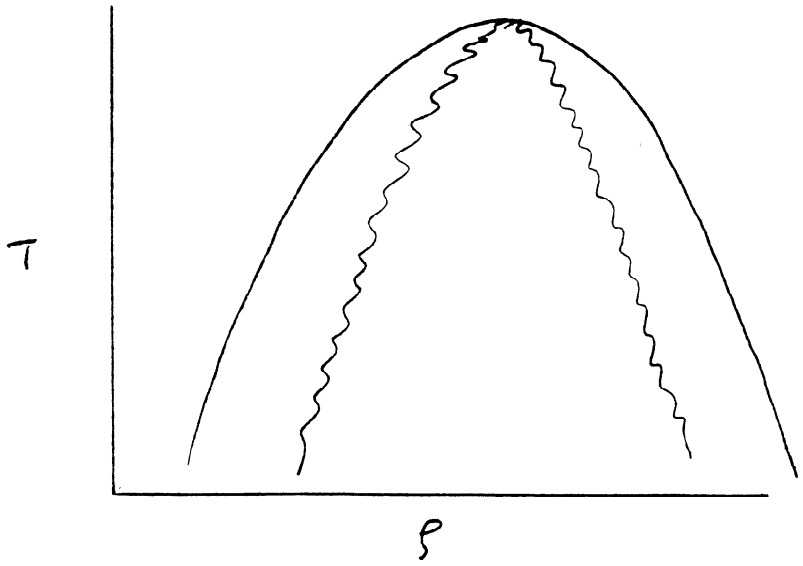

Fig. 11 Coexistence curve with Becker - Döring limit.

Three points must be stressed. First for many systems this limit of metastability is not the spinodal. Often there is no divergent susceptibility at this limit. Second, in such systems the limit is not a well defined line but is a crossover region with a finite width where one goes from quench depths where equilibrium ideas work well to one where they don't work at all. The spinodal at this point gives us a real problem. Since it is an equilibrium concept it can have no meaning past the limit of metastability nor can it exist between the Becker - Döring limit and the coexistence curve. For now we leave this as a question to be resolved when we return to nucleation with more powerful tools. Finally it is important to note that while I motivated treating the metastable state with equilibrium methods by the use of a mean - field theory the analysis that led to the classical nucleation theory was not mean field. There were, to be sure, several assumptions but they were not assumptions associated with the mean - field model.

Before leaving nucleation to consider the other problems we have set for ourselves let us look at a test of the classical theory. The test is a numerical simulation of a $d = 3$ nearest neighbor Ising model.[7] What do we measure? Remember that the probability of finding a critical droplet is τ^{-1} where τ is given by eq. 1.13. Consider a bit more carefully what this means. We have assumed that the critical droplets were non interacting. This assumption was based on the experimental observation that for shallow quenches the number of droplets is small enough so that they are well separated. Roughly there is a volume V inside which there is at most one droplet with probability τ^{-1}. Therefore τ^{-1} is the number of critical droplets per unit volume per unit time. This quantity is called the nucleation rate and is one of the variables measured in experiments.

Equation 1.13 gives us the classical prediction for the nucleation rate. In order to

compare the theory with the measurement we need to provide three factors; the constant of proportionality, the surface tension σ and ΔF_c The proportionality constant is too complicated for the theory at this level and will have to wait until we return to nucleation. However it is not important for the level of comparison of theory and experiment we will do now. The surface tension is, by assumption, not sensitive to the quench depth and therefore can be taken as the surface tension between two coexisting bulk phases.[7] Finally for ΔF_c we adopt the strategy that the free energy is well approximated by the energy for low temperatures. In this situatation the free energy difference between the two phases, stable and metastable is proportional to h. These considerations lead to the prediction that the log of number of critical droplets per unit volume per unit time when plotted against h^{-2} in $d = 3$ should be a straight line with a slope proportional to the surface tension. In fig. 12 I have reproduced[7] a plot of the log of the nucleation rate vs h^{-2} for $T = .59T_c$ As you can see the fit is not bad. There certainly are some questions, particularly about the deviations at small values of h but that is for another lecture. We turn now to spinodal decomposition and continuous ordering.

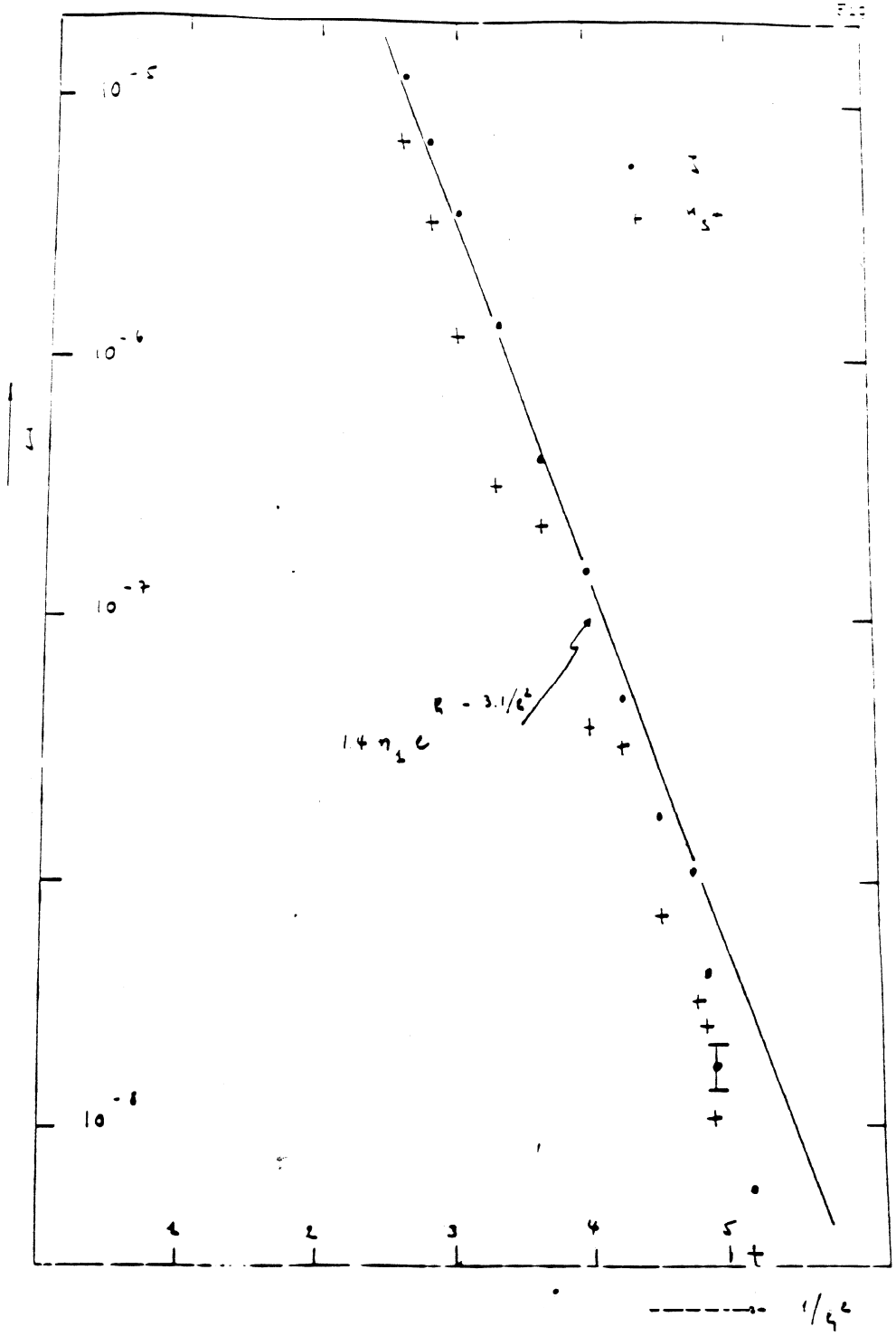

Fig. 12 Nucleation rate vs h^{-2} for a $d = 3$ nearest neighbor Ising model. The solid line is the classical theory prediction.

References Lesson I

1. *Thermodynamics* H. B. Callen (Wiley, New York 1960)

2. J. D. Gunton, M. San Miguel and P. S. Sahni in *Phase Transitions and Critical Phenomena Vol. 8* eds. C. Domb and J. L. Lebowitz (Academic Press, New york 1983)

3. *Statistical Physics* 3rd Edition Part 1, (Landau and Lifshitz Course of Theoretical Physics Vol. 5) E. M. Lifshitz and L. P. Pitaevskii, Pergamon, New York (1980)

4. *Modern Theory of Critical Phenomena*, S. K. Ma (Benjamin 1976)

5. *Statistical Mechanics*, K. Huang, Wiley (New York 1963)

6. *Phase Transitions and Critical Phenomena*, H. E. Stanley (Oxford 1971)

7. D. W. Heermann, A. Coniglio, W. Klein and D. Stauffer, J. Stat. Phys. **36**, 447 (1984)

Lesson 2

2.1 Introduction

The simple theory of nucleation made use of the idea that the metastable state is similar to an equilibrium state. When the quench brings the system into the unstable region equilibrium ideas no longer work as we saw with the van der Waals equation. Once this simplification is no longer possible we need to consider the laws governing the dynamical evolution. In this lesson we will concern ourselves with only two models. The first allows all extensive variables to fluctuate; ie. no extensive variables are conserved. Specifically the order parameter will be allowed to fluctuate. However, the system will be connected to a heat bath so that the temperature is fixed and hence the energy will also fluctuate. The second model we will consider will have only one conserved extensive quantity, the order parameter.

To investigate these dynamical models we will use the same coarse grained approach employed in the previous lesson. We will begin by considering the evolution of the order parameter, both local and global in the non - conserved model. If we were doing a thermodynamics problem in, for example, a one component fluid then the global order parameter would be the time dependent density and $\int \psi(\vec{x},t)d\vec{x} = \rho(t)$. From thermodynamics we know that

$$\frac{\partial \rho(t)}{\partial t} = -M\mu(t) \tag{2.1}$$

Where the proportionality constant is the mobility and $\mu(t)$ the time dependent chemical potential. Moreover,

$$\mu(t) = \frac{\partial F(\rho)}{\partial \rho(t)} \tag{2.2}$$

For the coarse grained model we will assume that these relations also hold so that

$$\frac{\partial \psi(\vec{x},t)}{\partial t} = -M\mu(\vec{x},t) \tag{2.3}$$

and

$$\mu(\vec{x}) = \frac{\delta F(\psi(\vec{x},t)}{\delta \psi(\vec{x},t))} \tag{2.4}$$

where the derivative in eq. 2.4 is the functional derivative and $F(\psi)$ is a functional of $\psi(\vec{x},t)$.

We will take as $F(\psi)$ eq. 1.7, the Landau - Ginsburg model. From eqs. 1.7, 2.3 and 2.4 we obtain

$$\frac{\partial \psi(\vec{x},t)}{\partial t} = -M\{-R^2\nabla^2 + 2\epsilon\psi(\vec{x},t) + 4\psi^3(\vec{x},t) - h\} \tag{2.5}$$

This dynamical model is usually refered to as Model A in the Hohenberg - Halperin classification.[1] or the Langevin equation for the non - conserved order parameter.[2]

For the conserved order parameter we must have

$$\frac{\partial\psi(\vec{x},t)}{\partial t} = M\nabla\cdot J(\psi) \tag{2.6}$$

where $J(\psi)$ is the current and

$$J(\psi) = \nabla\mu(\vec{x}) \tag{2.7}$$

Using eqs. 1.7, 2.4, 2.6 and 2.7 we obtain

$$\frac{\partial\psi(\vec{x},t)}{\partial t} = M\nabla^2\{-R^2\nabla^2\psi(\vec{x},t) + 2\epsilon\psi(\vec{x},t) + 4\psi^3(\vec{x},t)\} \tag{2.8}$$

This is Model B in the Hohenberg - Halperin classification.

Several comments are in order. First, eq. 2.6, the continuity equation, imposes a local conservation on the order parameter. Second, eqs. 2.5 and 2.8 are mean - field for the same reason that eq. 1.9 is mean - field. Finally, these equations are non - linear so that complicated behavior may result. We will be interested in the evolution of two quantities; the order parameter $\psi(\vec{x},t)$ which can be measured directly only in simulations and the correlation function

$$< \psi(\vec{x},t)\psi(\vec{x}',t) > - < \psi(\vec{x},t) >< \psi(\vec{x}',t) > \tag{2.9}$$

which can be related to scattering measurements. The <> refers to an ensemble average.

The quantity actually related to the experimental measurement is the structure factor $S(\vec{k},t)$ which is the Fourier transform of the correlation function. If the system is isotropic and the potential spherically symmetric then (see appendix 2.A)

$$S(\vec{k},t) \propto < \hat{\psi}(\vec{k},t)\hat{\psi}(-\vec{k},t) > \tag{2.10}$$

2.2 Continuous Ordering

We first consider continuous ordering for a critical quench. A critical quench is a quench at the critical ($m = 0$ in an Ising model) concentration if the order parameter conserved , or at $h = 0$ if it is not. All quenches will be instantaneous and in this lesson we will only consider the linear theory. With the critical quench we begin at $h = 0$ for $T > T_c$ and instantaneously lower the temperature to $h = 0$, $T < T_c$. The spatially averaged order parameter is $\psi = 0$ before the quench and is zero immediately after the quench. Note also

from eq. 1.19 that $\partial^2 f(\psi)/\partial\psi^2 < 0$ at $\psi = 0$ for $\epsilon < 0$ so that the system is unstable. We will investigate the initial evolution away from $\psi = 0$ described by $\psi(\vec{x},t) = u(\vec{x},t)$ which is assumed to be small throughout the time period we are studying. With this assumption we can linearize eq. 2.5

$$\frac{\partial u(\vec{x},t)}{\partial t} = -M\{-R^2\nabla^2 u(\vec{x},t) - 2|\epsilon|u(\vec{x},t)\} \tag{2.11}$$

where we have $T < T_c$ or $\epsilon < 0$.

We now assume

$$u(\vec{x},t) = \exp(\lambda t)\phi(\vec{x}) \tag{2.12}$$

Inserting eq. 2.12 into eq. 2.11 we obtain

$$\lambda\phi(\vec{x}) = M\{R^2\nabla^2\phi(\vec{x}) + 2|\epsilon|\phi(\vec{x})\} \tag{2.13}$$

From eq. 2.13

$$\lambda = -R^2k^2 + 2|\epsilon| \tag{2.14}$$

and

$$\phi(\vec{x}) \propto \exp[i\vec{k}\cdot\vec{x}] \tag{2.15}$$

where $k = |\vec{k}|$

The general solution to eq. 2.11 is

$$u(\vec{x},t) = \int c(\vec{k})e^{i\vec{k}\cdot\vec{x}}\exp[M(-R^2k^2 + 2|\epsilon|)t]d\vec{k} \tag{2.16}$$

where $c(\vec{k})$ are coefficients determined by the initial conditions. Modes with $R^2k^2 > 2|\epsilon|$ decay with time however, the modes with $R^2k^2 < 2|\epsilon|$ grow exponentially with time. This is the instability we have been seeking and the reason that equilibrium methods do not work in the unstable region. For t very large the $k = 0$ mode dominates the growth. We have assumed of course that the linear theory is valid for such large times.

What is happening to the structure factor? From the above discussion

$$\hat{u}(\vec{k},t) = c(\vec{k})\exp[(-R^2k^2 + 2|\epsilon|)t] \tag{2.17}$$

In the linear approximation for a critical quench

$$S(\vec{k},t) \propto < \hat{u}(\vec{k},t)\hat{u}(-\vec{k},t) > \tag{2.18}$$

or

$$S(\vec{k},t) \propto < c(\vec{k})c(-\vec{k}) > \exp[2(-R^2k^2 + 2|\epsilon|)t] \tag{2.19}$$

Since the quench is instantaneous the structure at $t = 0$ is the structure of the equilibrium state before the quench. Therefore $< c(\vec{k})c(-\vec{k}) >$ is the equilibrium structure factor at the start of the quench. Note that the expression $\exp(D(k)t)$, which will be called the amplification factor, appears in the evolution of both the order parameter (eq. 2.16) and the structure factor (eq. 2.18) with

$$D(k) = -R^2k^2 + 2|\epsilon| \tag{2.20}$$

Equation 2.19 implies that after the quench the structure factor which describes the equilibrium state at the start of the quench simply becomes amplified by $\exp[(-R^2k^2 + 2|\epsilon|)]$. Clearly there is something wrong here. To see the problem consider quenching from $T = \infty$ where the equilibrium structure factor is zero. Our result would imply that the structure factor would remain zero for all t after the quench. This is clearly nonsense. What then is the problem? The problem is that we have neglected fluctuations. In our formulation of the equations of motion we have used the Landau - Ginsburg free energy and that is not good enough. To see why, we need to take a closer look at mean - field theories.

2.3 Mean - field Digression

As I have said before there are many ways to get to mean - field theories. The one that we will use was first proposed by Kac, Uhlenbeck and Hemmer and refined by Lebowitz and Penrose.[3] We will consider the Ising model in the lattice gas representation but we will impose as well the conservation of particles. In Ising spin language that means we sum over all configurations consistent with a fixed magnetization. We will use fluid language so that the partition function in the Canonical ensemble is given by

$$Z = (N!)^{-1} \int d\{\vec{x}_i\} \exp[\sum_{ij} K(x_{ij})] \tag{2.21}$$

We now take

$$K(x_{ij}) = \gamma^d v(\gamma x_{ij}) \tag{2.22}$$

where $\gamma = R^{-1}$ and there are no restrictions on $v(\gamma x_{ij})$ except

$$\int \gamma^d v(\gamma x) d\vec{x} = 1 \tag{2.23}$$

Note that eq. 2.23 can be crudely interpreted to mean that the integral kills the γ^d. More precisely the length scale of the lattice spacing is no longer the fundemental physical length

scale, it is now $\gamma^{-1} = R$ and all lengths must be scaled with the interaction range. In our Ising model/Lattice gas discussion we will also take $v(\gamma x_{ij}) \geq 0 \ \forall \ i,j$

We also define

$$f(x_{ij}) = \exp[K(x_{ij})] - 1 \tag{2.24}$$

the so called Mayer function.[4] With this definition the partition function can be written as

$$Z = (N!)^{-1} \int d\{\vec{x}_i\} \prod_{i \neq j} [f(x_{ij}) + 1] \tag{2.25}$$

We can now expand the product in eq. 2.25 and write the partition function as a sum of products of Mayer functions. We can also group the terms in the expanded product into classes. For example there is a term in the partition function that has the form

$$\int d\{\vec{x}_i\} \sum_{pairs} f(x_{ij}) \tag{2.26}$$

which is equal to

$$\frac{V^N}{2} \rho \int d\vec{x} f(x) \tag{2.27}$$

for large number of particles N. In eq. 2.27 V is the volume and ρ the number density.

In this way the partition function can be written as a sum of products of Mayer functions which are generic that is the terms do not refer to specific particles but can be grouped into 2 particle graphs, three particle graphs etc. However this classification is not quite good enough. To see this we first introduce Mayer graphs. In a Mayer graph each vertex corresponds to a particle and each line to a $f(x)$ which will also be referred to as a Mayer bond as well as a Mayer function. For example the term $f(x_{12})$ is represented by the graph in fig. 2.1. Within the classes of e. g. three particle graphs there are two distinct subclasses which are topologically different. One three particle graph corresponding to $f(x_{12})f(x_{23})$ is given in fig.2.2a and the other corresponding to $f(x_{12})f(x_{13})f(x_{23})$ is given in fig. 2.2b. Note that the number of lines is equal to the number of Mayer functions or bonds in the expansion of the partition function and the number of verticies minus one is equal to the number of restricted integrals left to perform. A restricted integral are those which do not range over the entire volume but are restricted by the range of the potential through the Mayer function.

We now take for $K(x_{ij})$ the Kac potential in eq. 2.22. The Mayer function is now expanded in a power series in γ^d.

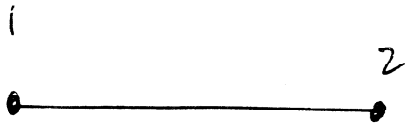

Fig. 2.1 Diagram corresponding to $f(x_{12})$

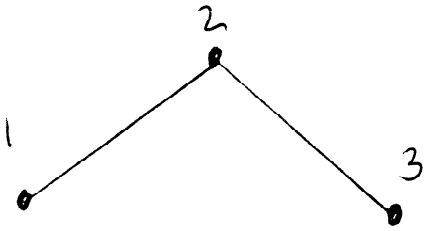

Fig. 2.2a Diagram for $f(x_{12})f(x_{23})$

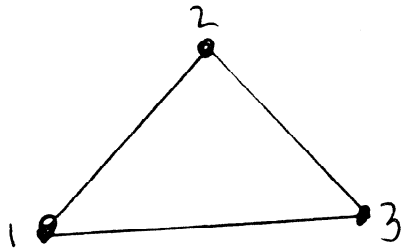

Fig. 2b Diagram for $f(x_{12})f(x_{13})f(x_{23})$

Keeping only up to first order in γ^d each Mayer function $f(x) = \gamma^d v(\gamma x)$. Consequently in our graphical representation each line in the graph carries a weight proportional to γ^d. In our expression for the partition function all particles, and hence all verticies imply an integral. As discussed after eq. 2.23 each integral "kills" a factor of γ^d. Or more precisely, each restricted integral when rescaled absorbs a factor γ^d in the rescaling. The only graphs that contibute then to zeroth order in γ^d are tree graphs, i. e. graphs with no loops. Each loop implies one more Mayer bond than integral and hence an non killed (or rescaled) factor of γ^d. For mean - field thermodynamics then the dominant contribution, in fact the only contribution in the limit $\gamma \to 0$, comes from tree graphs.

What about fluctuations? Fluctuations imply correlations. We can see that from the correlation function in eq. 2.9. If there are no fluctuations then $< \psi(\vec{x}) >= \psi(\vec{x})$ since there is only one state. Moreover, $< \psi(\vec{x})\psi(\vec{x}') >= \psi(\vec{x})\psi(\vec{x}')$ for the same reason. From eq. 2.9 the correlation function is zero. Hence, no fluctuations - no correlations.

What is the correlation function in our lattice gas model with a Kac potential? The correlation function in fluid language is simply the probability that there is a paritcle at $\vec{x}_1$ given that there is a particle at $\vec{x}_2$ $(\rho_2(\vec{x}_1, \vec{x}_2))$ minus the probability that there is a

particle at $\vec{x}_1$ ($\rho_1(\vec{x}_1)$) times the probability there is a particle at $\vec{x}_2$. Where

$$\rho_2(\vec{x}_1, \vec{x}_2) = \frac{1}{N!} \frac{\int d\vec{x}_3 \cdots d\vec{x}_N \exp[\sum_{ij} K(x_{ij})]}{Z} \tag{2.28}$$

and

$$\rho_1(\vec{x}_1) = \frac{1}{N!} \frac{\int d\vec{x}_2 \cdots d\vec{x}_N \exp[\sum_{ij} K(x_{ij})]}{Z} \tag{2.29}$$

and Z is given by eq. 2.21. There is a similar expression for $\rho_1(\vec{x}_2)$ with the obvious changes.

Graphical expansions can be developed for $\rho_2(\vec{x}_1, \vec{x}_2)$ and $\rho_1(\vec{x}_1)$ in the same way as we did for the partition function with two significant differences. These graphs will contain root points, that is verticies that are not integrated. This clearly follows from the absence of integration over particles 1 and 2 in eq. 2.28 and particle 1 in 2.29. The second important difference is that the only graphs that give a non - zero contribution to the **correlation function** are graphs that connect particles 1 and 2. This can be proven[5] however, it is easy to see that it must be so. If the distance $|\vec{x}_1 - \vec{x}_2|$ is taken to infinity then there will be no correlation between particles 1 and 2. This implies that

$$\lim_{|\vec{x}_1 - \vec{x}_2| \to \infty} \rho_2(\vec{x}_1, \vec{x}_2) - \rho_1(\vec{x}_1)\rho_1(\vec{x}_2) = 0 \tag{2.30}$$

However, the only graphs that are affected by the separation of particles 1 and 2 are those that connect these two particles via Mayer bonds. Since all graphs give a zero contribution when $|\vec{x}_1 - \vec{x}_2| = x_{12} \to \infty$ those that are independent of x_{12} must give zero contribution for all values of x_{12}.

From this discussion all graphs associated with the pair correlation function in eq. 2.9 have at least one factor of γ^d. Consider for example the graph in fig. 3 which appears in the expansion of the pair correlation function. The root points are designated by open circles and they stand for particles 1 and 2. These points do not get integrated. The filled circle is called a field point and all field points indicate an integral. As before all bonds stand for a Mayer function and hence in the case of the Kac potential contribute a factor of γ^d. The graph in fig. 3 then has two Mayer bonds but only one field point or integral and hence is of order γ^d. To zeroth order then correlation functions are zero and hence there are no fluctuations.

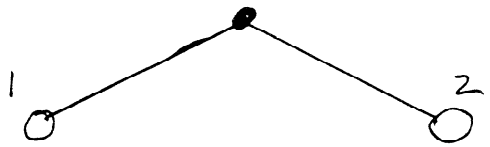

Fig. 2.3 Term in graphical expansion of the pair correlation function. Open circles are root points and filled circles field points.

However, this is not quite the whole story. The static structure factor $S(\vec{k})$ which is the time independent, equilibrium version of eq. 2.10 is related to the isothermal compressibility κ_T via

$$\lim_{\vec{k}\to 0} S(\vec{k}) \propto \kappa_T \tag{2.31}$$

But the integral in the Fourier transform used to obtain the structure factor from the correlation function killed a factor of γ^d so that the isothermal compressibility in eq. 2.31 is of zeroth order. In other words the correlation function to order γ^d describes the isothermal compressibility and structure factor to order zero in γ^d. Hence if we wish to describe the experimental measurements of the structure factor, even in a mean - field contex, we must include fluctuations in our description of the correlation function.

The simplest way to do this is to add a term to the Landau - Ginsburg free energy of the form

$$\int \eta(\vec{x},t)\psi(\vec{x},t) \tag{2.32}$$

where $\eta(\vec{x},t)$ is a Gaussian random noise. The only restrictions on $\eta(\vec{x},t)$ are

$$< \eta(\vec{x},t) >= 0 \tag{2.33}$$

and

$$< \eta(\vec{x},t)\eta(\vec{x}',t') >= K_B T\delta(\vec{x}-\vec{x}')\delta(t-t') \tag{2.34}$$

2.4 Return to Continuous Ordering

In order to obtain $u(\vec{x},t)$ we must solve

$$\frac{\partial u(\vec{x},t)}{\partial t} = -M\{-R^2\nabla^2 u(\vec{x},t) - 2|\epsilon|u(\vec{x},t)\} + \eta(\vec{x},t) \tag{2.35}$$

instead of eq. 2.11. The solution, of course, is the sum of two terms. One is the solution to the homogeneous equation and is given in eq. 2.16. The second is the solution to the inhomogeneous equation and can best be obtained by going into Fourier space with eq. 2.35. That is we wish to solve

$$\frac{\partial \hat{u}(\vec{k},t)}{\partial t} = M\{-R^2k^2\hat{u}(\vec{k},t) + 2|\epsilon|\hat{u}(\vec{k},t)\} + \hat{\eta}(\vec{k},t) \tag{2.36}$$

The homogeneous solution to eq. 2.36 is given by eq. 2.17. To obtain the inhomogeneous solution we solve for the Green's function

$$\frac{\partial G(t,t')}{\partial t} + M\{R^2k^2 - 2|\epsilon|\}G(t,t') = \delta(t-t') \tag{2.37}$$

Taking the Fourier transform with respect to time gives

$$\hat{G}(\omega) = \frac{e^{-i\omega t'}}{i\omega + M\{R^2k^2 - 2|\epsilon|\}} \tag{2.38}$$

Inverting the Fourier transform we obtain

$$G(t,t') = \frac{-i}{2\pi}\int \frac{e^{i\omega(t-t')}}{\omega - iM\{R^2k^2 - 2|\epsilon|\}}d\omega \tag{2.39}$$

We do the inversion as a contour integral. Imposing the causality condition (retarded Green's function) so that $t > t'$ we close the contour in the upper half plane for $R^2k^2 > 2|\epsilon|$ and analytically continue to values of k for which $R^2k^2 < 2|\epsilon|$. We obtain

$$G(t,t') = G(t-t') = \exp[-(t-t')M(R^2k^2 - 2|\epsilon|)] \tag{2.40}$$

The solution to eq. 2.36 is

$$\hat{u}(\vec{k},t) = \hat{c}(\vec{k})\exp[M(-R^2k^2 + 2|\epsilon|)t] + \int_0^t \eta(\vec{k},t')G(t-t')dt' \tag{2.41}$$

In order to obtain the structure factor we again form the product $V^{-1} < \hat{u}(\vec{k},t)\hat{u}(\vec{k}',t) >$ where we have made the V^{-1} term explicit (see appendix). From eq. 2.41

$$\begin{aligned} V^{-1} < \hat{u}(\vec{k},t)\hat{u}(\vec{k}',t) > &= V^{-1} < \hat{c}(\vec{k})\hat{c}(-\vec{k}) > \exp\{2D(k)t\} + \\ &V^{-1}\int_0^t\int_0^t < \eta(\vec{k},t')\eta(-\vec{k},t'') > G(t-t')G(t-t'')dt'dt'' \end{aligned} \tag{2.42}$$

where we have used eq. 2.33 to eliminate the cross terms.

From eq. 2.34 and the discussion in the appendix 2.A

$$V^{-1} < \eta(\vec{k},t')\eta(-\vec{k},t'') >= K_B T\delta(t'-t'') \tag{2.43}$$

Using eq. 2.43 and 2.40 eq. 2.42 becomes

$$S(k,t) = S_0(k)\exp\{2D(k)t\} + \frac{1}{2D(k)}[\exp\{2D(k)t\} - 1] \tag{2.44}$$

where we have set $S_0(k) = V^{-1} < \hat{c}(\vec{k})\hat{c}(-\vec{k}) >$ to make explicit that for instantaneous quenches this term is the equilibrium structure factor at the point where the quench initiated.

Now we have something that makes sense. The first term in eq. 2.44 is the Cahn - Hilliard term[2,6,7] which describes the evolution of modes present in the system at the quench. The second term in eq. 2.44 is the Cook[2,8] term which tells us how the modes associated with the fluctuations present at the quench temperature evolve.

Two final points.; The time scale for the evolution described by eq. 2.44 is set by $D(k)$ and hence by $|\epsilon|$. If $\epsilon \rightarrow 0$, i. e. we approach the critical point, then the growth of the unstable modes slows down. Since the mode at $k = 0$ grows fastest we have that the characteristic time $\tau \sim \epsilon^{-1} \propto \xi^2$ where ξ is the correlation length. This is an example of critical slowing down. In general near critical point $\tau \sim \xi^z$ where z is different from 2. The value of $z = 2$ is the mean - field result for model A. The second point is that the off critical quench is more difficult to describe. The reason is that in addition to the small perturbation there is a large amplitude $k = 0$ mode for small time that cannot be treated linearly. For that reason we will put off our discussion of off critical quenches to a later lesson and consider next spinodal decomposition for both crtical and off critical quenches.

2.5 Spinodal decomposition

Spinodal decomposition is the evolution of a system quenched into the unstable region when the order parameter is conserved. To describe this evolution we return to eq. 2.8. However we must add a noise term as we discussed in the case of continuous ordering. Cosequently we must solve the equation

$$\frac{\partial\psi(\vec{x},t)}{\partial t} = M\nabla^2\{-R^2\nabla^2\psi(\vec{x},t) - 2|\epsilon|\psi(\vec{x},t) + 4\psi^3(\vec{x},t)\} + \eta(\vec{x},t) \tag{2.45}$$

where $\eta(\vec{x},t)$ satisfies eq. 2.33 and

$$< \eta(\vec{x},t)\eta(\vec{x}',t') >= -K_B T\nabla^2\delta(\vec{x}-\vec{x}')\delta(t-t') \tag{2.46}$$

The proceedure we will follow is almost identical to the case of continuous ordering. We first linearize by assuming

$$\psi(\vec{x},t) = \psi_0 + w(\vec{x},t) \tag{2.47}$$

where $w(\vec{x},t)$ is assumed to be small throughout the time period we are studying. Inserting eq. 2.47 into eq. 2.45 and keeping only terms linear in $w(\vec{x},t)$ we obtain

$$\frac{\partial w(\vec{x},t)}{\partial t} = M\nabla^2\{-R^2\nabla^2 w(\vec{x},t) - 2|\epsilon|w(\vec{x},t) + 12\psi_0^2 w(\vec{x},t)\} + \eta(\vec{x},t) \tag{2.48}$$

Equation 2.48 can be solved with the same methods used in the case of continuous ordering. For the order parameter we obtain

$$\hat{w}(\vec{k},t) = \hat{d}(k)\exp[\tilde{D}(k)t] + \int_0^t \eta(\vec{k},t')\tilde{G}(t-t')dt' \tag{2.49}$$

where

$$\tilde{D}(k) = -k^2[R^2k^2 - 2|\epsilon| + 12\psi_0^2] \tag{2.50}$$

and

$$\tilde{G}(t-t') = exp[(t-t')\tilde{D}(k)] \tag{2.51}$$

For the structure factor

$$S(k,t) = S_0(k)\exp[2\tilde{D}(k)t] + \frac{1}{2\tilde{D}(k)}\{\exp[2\tilde{D}(k)t] - 1\} \tag{2.52}$$

Comparing eqs. 2.44 and 2.52 we see that the only difference is in the form of the functions $D(k)$ and $\tilde{D}(k)$ given in eqs. 2.20 and 2.25 respectively. In the case of continuous ordering the fastest growing mode is at $k = 0$ In contrast, the fastest growing mode (for large t) in spinodal decomposition is at

$$k^2 = \frac{|\epsilon| - 6\psi_0^2}{R^2} \tag{2.53}$$

Both theories predict that the growth of the structure factor is exponential. The differences at this point appear to be minor but, as we shall see, the later time evolution which must be described by a non - linear theory is quite different. We shall also see that even in the linear regime there are significant differences.

A final note; We have been discussing the linear theory where $u(\vec{x},t) << 1$. The linear theory will not be valid for all times. In fact, as we shall see, the interval of time for which it is valid depends on the material or system under study. Some materials will be properly

described by the linear theory up to $t_0 >> 1$ but for others it is not clear that there is any time that the linear theory is valid.

2.6 Experimental Data

Below we plot the structure factor as a functon of k for various times. The data was taken for a two dimensional Ising model with several values of the interaction range. The parameter q is the number of spins with which one spin interacts. Figure 2.4 is for continuous ordering and 2.5 for spinodal decomposition. In figs. 2.6 and 2.7 is plotted the structure factor as a function of time for various vakues of k. The parameter n is related to k via $k = 2\pi n/256$ where 256x256 is the lattice size. The dots are the data and the lines are the linear theory. These figures are taken from Laradji's thesis.

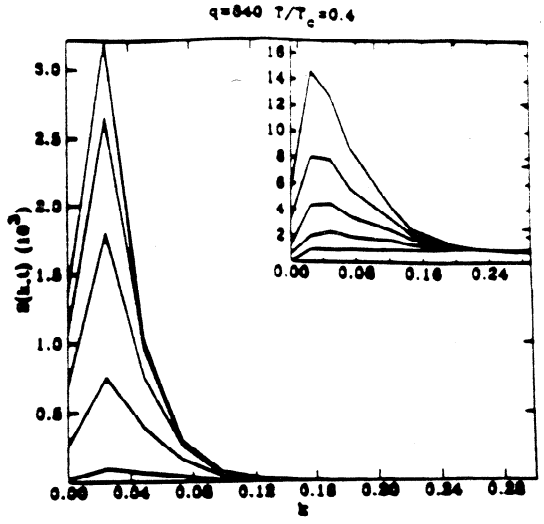

Fig. 2.4 $S(k,t)$ as a function of k for several times in a continuous ordering process. The finite value of k at the peak is due to finite system size.

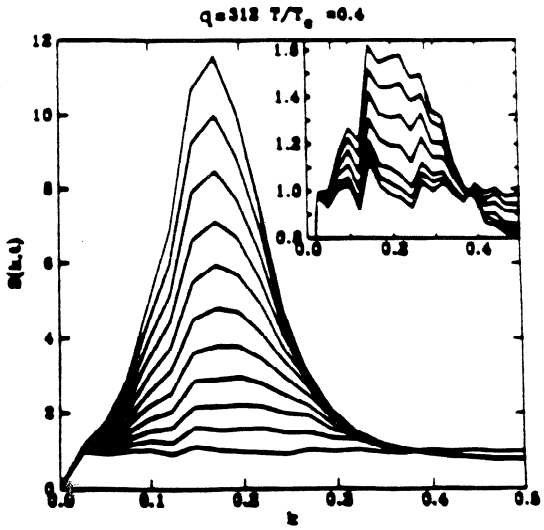

Fig. 2.5 $S(k,t)$ as a function of k for several times in a spinodal decomposition process.

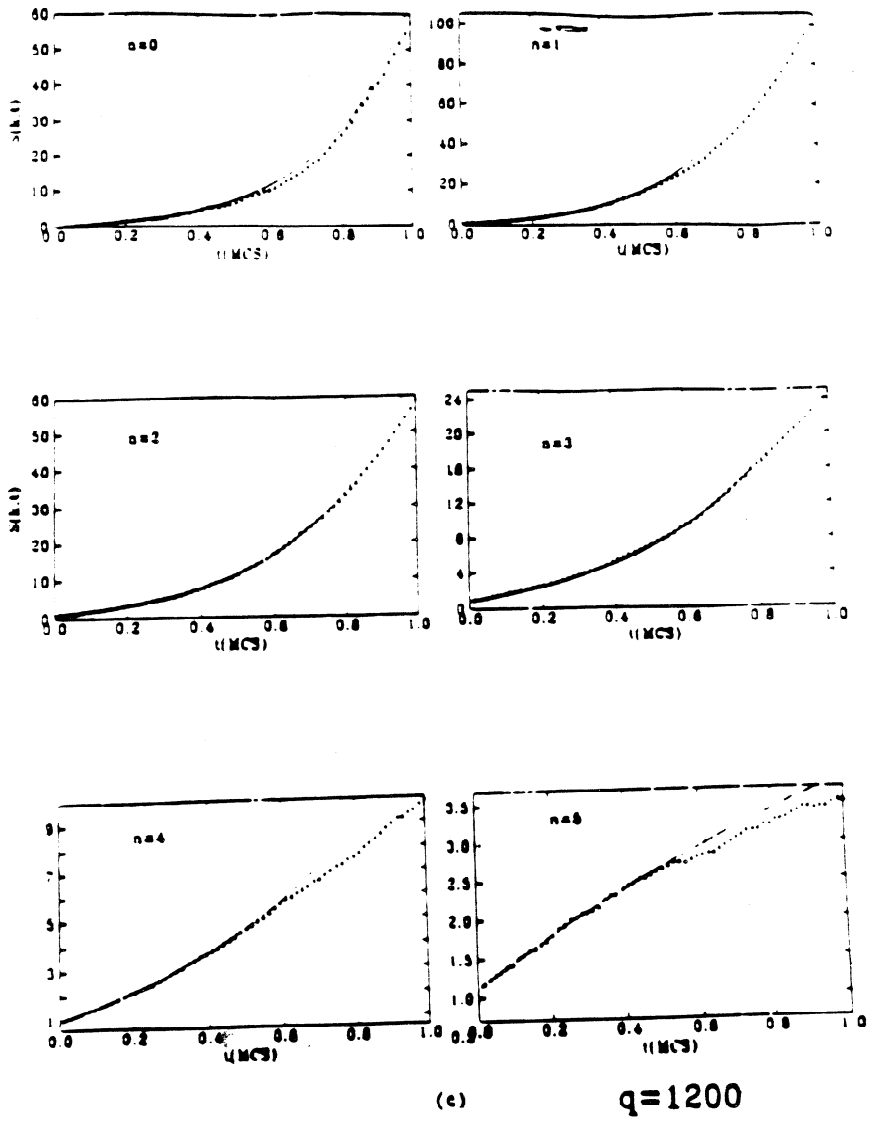

Fig. 2.6 $S(k,t)$ as a function of time for several values of k in a continuous ordering process.

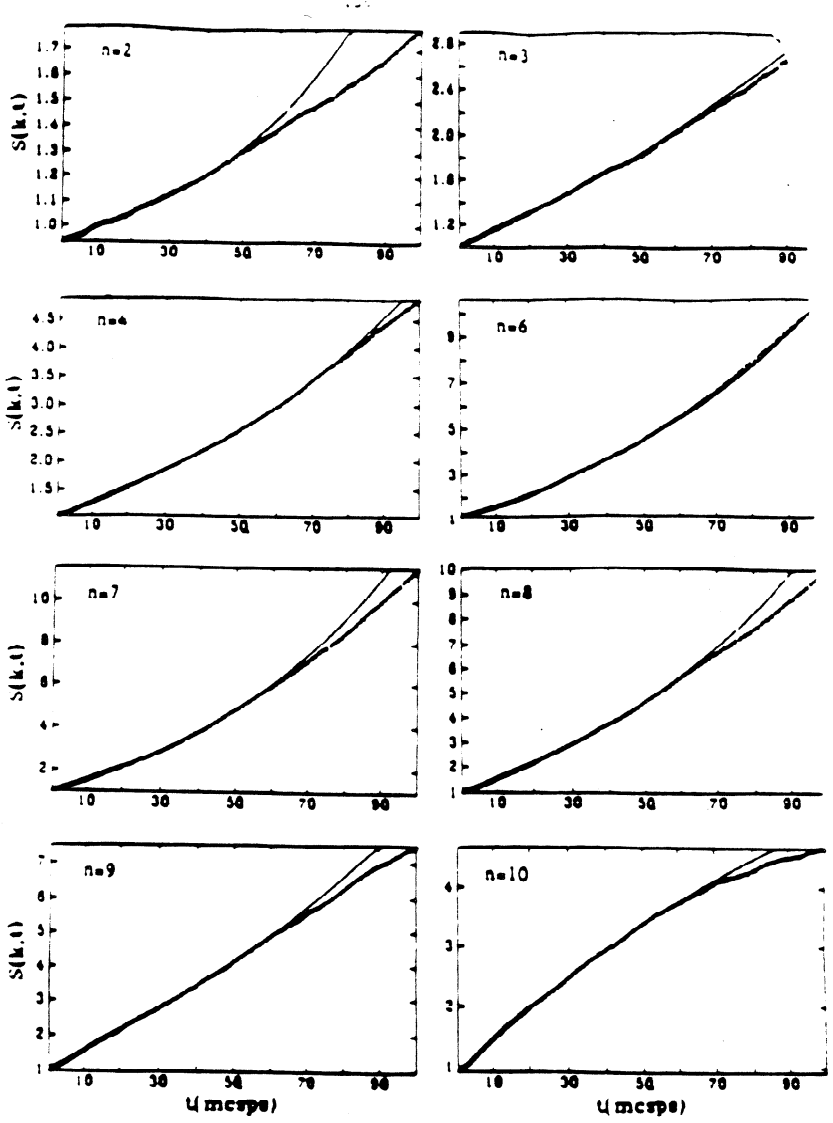

Fig. 2.7 $S(k,t)$ as a function of time for several values of k in a spinodal decomposition process.

References Lesson 2

1. P. Hohenberg and B. I. Halperin, Rev. Mod. Phys. **49**, 435 (1977)
2. See ref. 2 in Lesson 1
3. O. Penrose and J. L. Lebowitz in *Fluctuation Phenomena*, E. W. Montroll and J. L. Lebowitz eds. (North - Holland 1976) and references therein.
4. T. Hill, *Statistical Mechanics* (McGraw - Hill, New York 1956)
5. G. Stell in *The Equilibrium Theory of Classical Fluids*, H. L. Frisch and J. L. Lebowitz eds. (Benjamin, New York, 1964)
6. J. W. Cahn and J. E. Hilliard, J. Chem. Phys. **31**, 688 (1959)
7. J. W. Cahn, Acta Metall. **9**, 795 (1961)
8. H. E. Cook, Acta Metall. **18**, 297 (1970)

Appendix 2.A

The structure factor is related to the Fourier transform of the pair correlation function. Let

$$g(\vec{x},\vec{x}',t) =< \psi(\vec{x},t)\psi(\vec{x}',t) > - < \psi(\vec{x},t) >< \psi(\vec{x}',t) > \qquad (2.A.1)$$

For the problems we are interested in this lecture the ensemble average

$$< \psi(\vec{x},t) >= \rho(t) \qquad (2.A.2)$$

which is time dependent but spatially constant. Consequently there will be delta functions, $\delta(\vec{k})$ arising from the Fourier transform of the two terms on the right hand side of eq. 2.A.1. These delta functions will cancel. We will deal with this $\vec{k} = 0$ divergence by ignoring the term $< \psi(\vec{x},t) >< \psi(\vec{x}',t >$ but always taking the limit $\vec{k} \rightarrow 0$ when investigating the $\vec{k} = 0$ mode in the structure factor.

For a system with spherical symmetry we know that

$$g(\vec{x},\vec{x}',t) = g(|\vec{x} - \vec{x}'|,t) \qquad (2.A.3)$$

The structure factor in this case is given by

$$S(|\vec{k}|,t) = V^{-1} \int g(|\vec{x} - \vec{x}'|)e^{-i\vec{k}\cdot(\vec{x}-\vec{x}')} d(\vec{x} - \vec{x}')d\vec{x}' \qquad (2.A.4)$$

where the integral over $\vec{x}'$ simply produces a factor V.

We can also write eq. 2.A.4 as

$$S(k,t) = V^{-1} \int g(|\vec{x} - \vec{x}'|)e^{-i\vec{k}\cdot\vec{x}} e^{-i\vec{k}'\cdot\vec{x}'} \delta(\vec{k} + \vec{k}')d\vec{x}d\vec{x}'d\vec{k}' \qquad (2.A.5)$$

where $k = |\vec{k}|$

From the discussion above we can replace $g(|\vec{x} - \vec{x}'|)$ with $< \psi(\vec{x})\psi(\vec{x}') >$ so that eq 2.A.5 becomes

$$S(k,t) = V^{-1} \int < \psi(\vec{x})\psi(\vec{x}') > e^{-i\vec{k}\cdot\vec{x}} e^{-i\vec{k}'\cdot\vec{x}'} \delta(\vec{k} + \vec{k}')d\vec{x}d\vec{x}'d\vec{k}' \qquad (2.A.6)$$

or

$$S(k,t) = V^{-1} < \hat{\psi}(\vec{k})\hat{\psi}(-\vec{k}) > \qquad (2.A.7)$$

Remember at $k = 0$ there is a delta function $(\delta(\vec{k}))$ singularity we are ignoring.

Lesson 3

3.1 Introduction

As we have said several times the theories presented in lessons 1 and 2 are not incorrect but have limited validity. The aim of the next few lectures is to develop theories with a wider range of validity for nucleation, spinodal decomposition and continuous ordering. What is wrong with the theories we have discussed so far? Since this lesson and the next two or three will concentrate on nucleation, we will limit our remarks here to the completeness and validity of the classical theory of nucleation discussed in lesson 1.

The first point that should be stressed is that experimental data, that is to say, real experiments do not see the critical droplets. At this time experimentalists measure nucleation rates by counting the number of droplets that they can see per unit volume per unit time. However, since those droplets are much bigger than critical, experimentalists must hope that the density of droplets is low enough that there is no coalesence during the growth phase. With this undertstanding we point out that there are many experiments that agree with the classical theory in that the nucleation rate scales with quench depth as predicted in eqs. 1.12 and 1.13. However there are several experiments where the quench depth dependence is not predicted by the classical theory. It is , of course, extremely difficult to contol all of the factors in real experiments so it is hard to know just how bad the disagreement is with the classical theory. These topics will be discussed in Lesson 4.

There are however other reasons to believe that the classical theory as presented in Lesson 1 is incomplete and not universally valid. First, in fig. 3.1 we have plotted the log of the nucleation rate as a function of h^{-2} for the same Ising model[1] as in fig. 1.12. with the single difference being the temperature. The temperature in fig. 1.12 is $0.59T_c$ and that in fig. 3.1 is $0.86T_c$. Note the curvature in fig. 3.1 as well as the difference in the magnitude of the rates. In fig. 3.2 we plot the log of the nucleation rate as a function of h^{-2} again for the same Ising model as in fig. 1.12 but now we have used a different dynamics.[2] The crosses, open circles and triangles are taken for different system sizes using a different algorithm known as the Swendsen-Wang algorithm.[3] The only difference between the Swendsen-Wang dynamics and Metropolis is that clusters rather than single spins are flipped. The closed circles are the data in fig. 1.12 repeated to facilitate comparison. Note again the change in the position of the line of data. It would appear that these two simple changes; temperature and dynamics lead to a change in nucleation rate not predicted by the simple theory in Lesson 1.

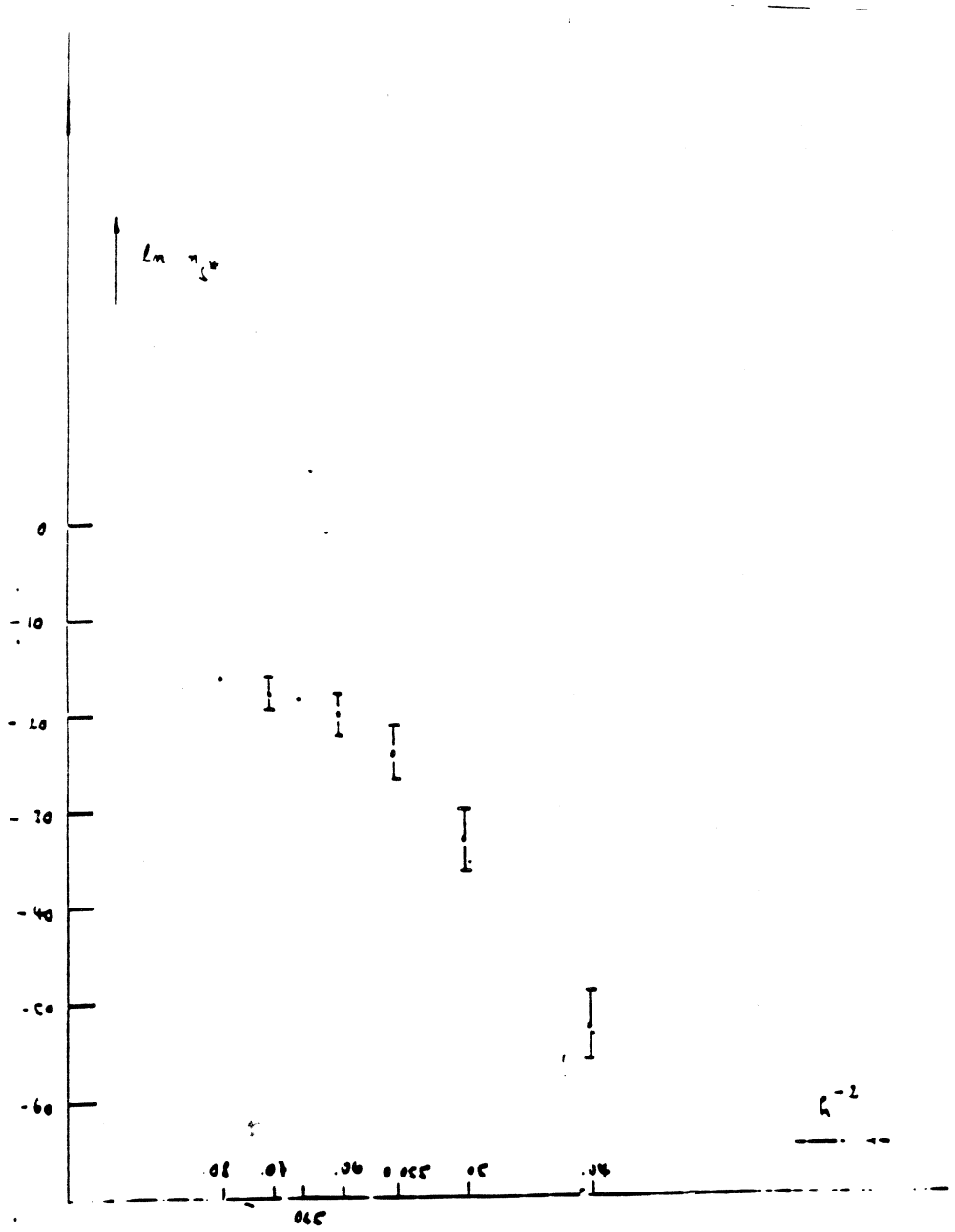

Fig. 3.1 Log of the nucleation rate as a function of h^{-2} for a $d = 3$ Ising model at $T = 0.86T_c$

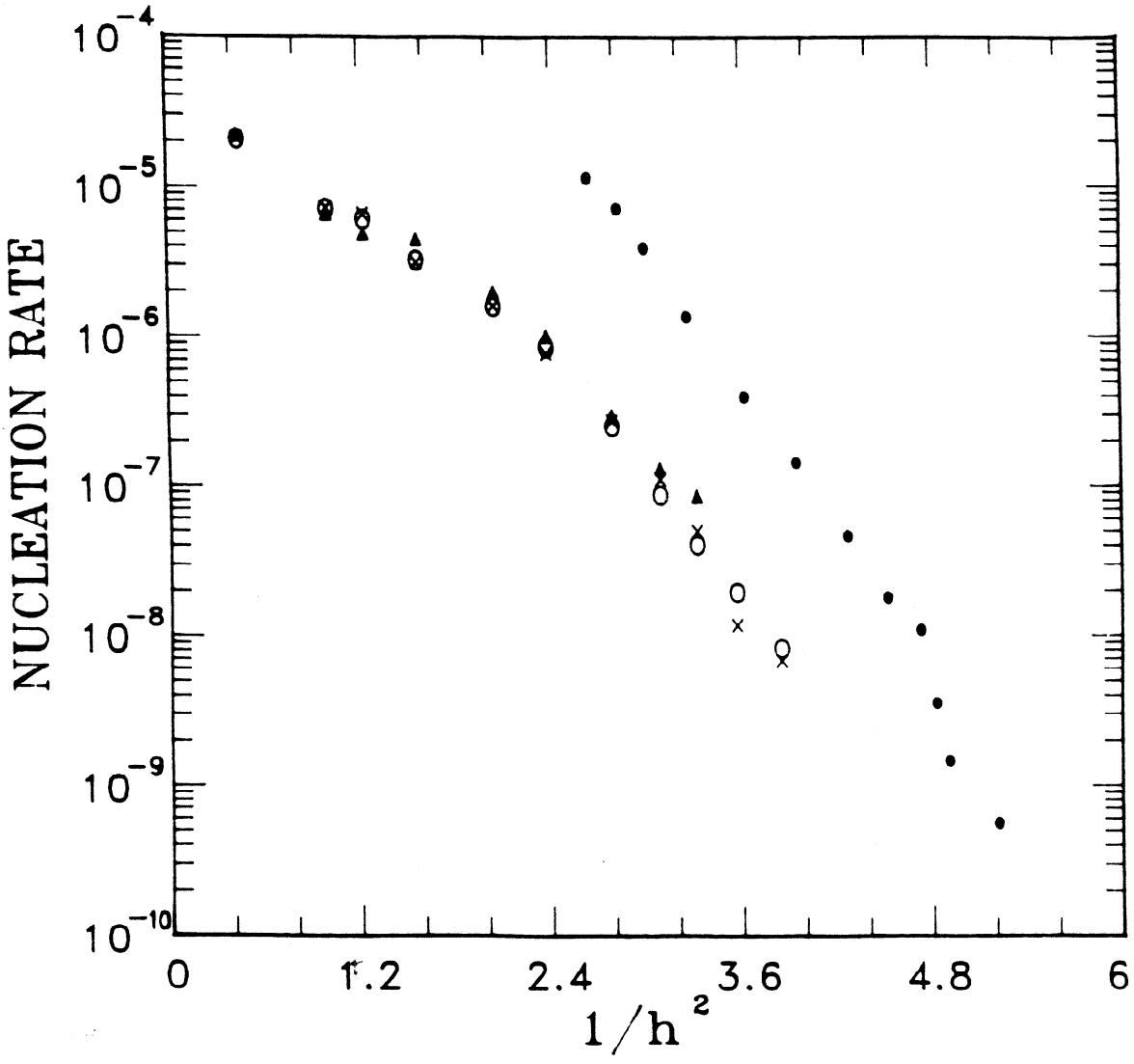

Fig. 3.2 Log of the nucleation rate as a function of h^{-2} for a $d = 3$ Ising model at $0.59T_c$ simulated with the Swendsen-Wang cluster algorithm.

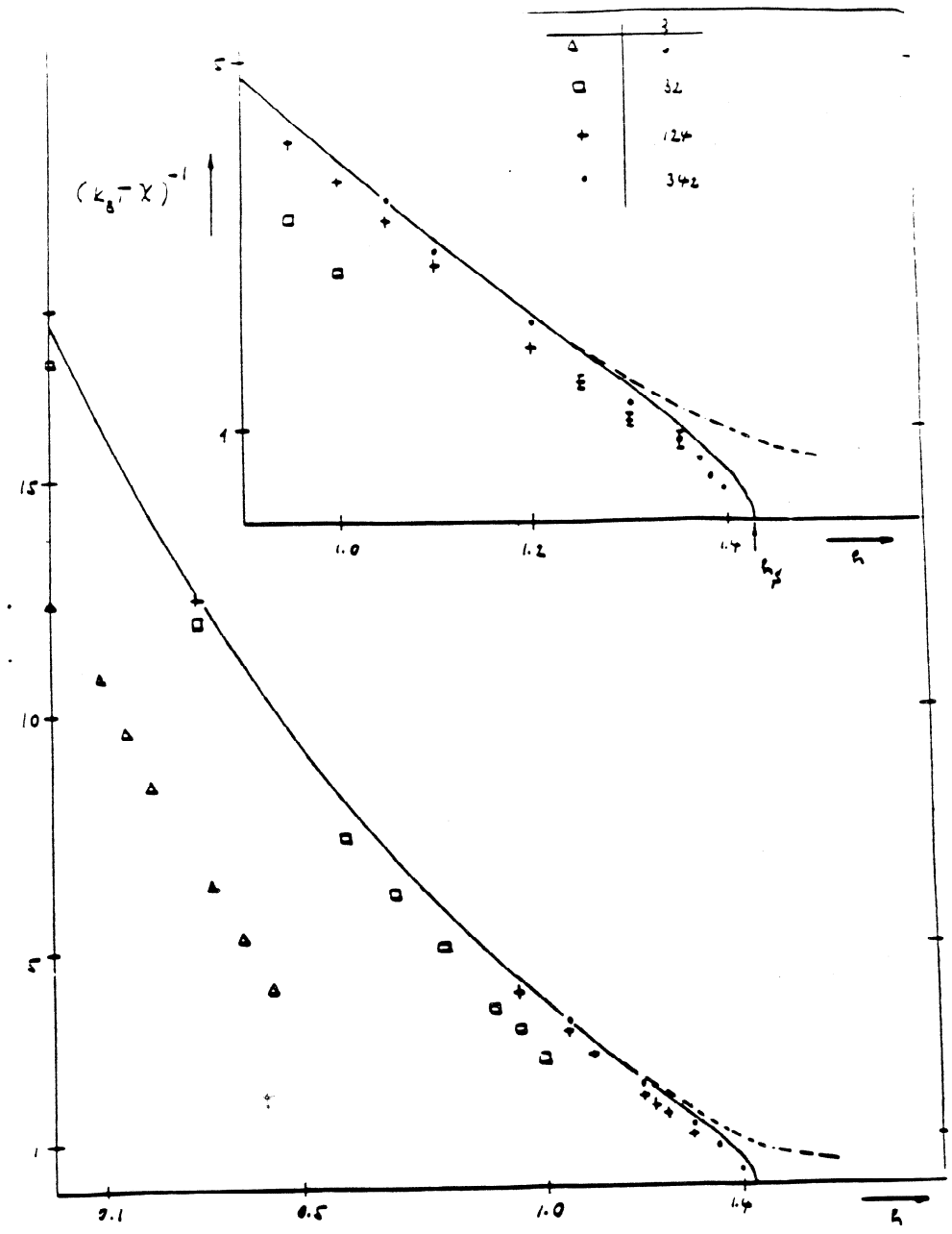

Fig. 3.3 Inverse isothermal susceptibility vs magnetic field for Ising model with various interaction ranges.

There are other problems with the simple theory as well. For example, there is a strong assumption about the shape of the critical droplet. One would like to see this assumption obtained starting from more basic principles. Second it is not at all clear that this basic assumption is true. For example lets return to the mean - field model discussed in lesson 1. Mean - field descriptions of Ising models become exact in the limit of long range interactions[4]. In such long range models spinodals become precisely defined. This is illustrated in fig. 3.3 in which we have plotted the inverse isothermal susceptibility for Ising models with different interaction ranges.[5] The precise model we use has each spin at the center of a cube ($d = 3$) or square ($d = 2$) of side L. The spin at the center of the cube has an interaction which is zero with spins outside of the cube but the center spin interacts with each spin in the cube with a strength.

$$K = \frac{J}{K_B T q} \tag{3.1}$$

where $q = L^d$ is the number of spins one spin interacts with. This is known as the Domb - Dalton model.[6]

For $q = 6$ the interaction is nearest neighbor in the simple cubic lattice used in our simulations. Note that there is really no sign of a spinodal in the nearest neighbor model. As q, and hence the interaction range, increases the model becomes more mean - field. This can be seen by comparing the data to the solid line which is the exact solution as $q \to \infty$. The isothermal compressibility diverges as the spinodal is approached similar to the behavior at a critical point. The surface tension will also vanish.[6] This presents two difficulties for the classical theory. First, the surface tension cannot be what is preventing nucleation if it is vanishing. Second, droplets, or any large fluctuations, should not be compact objects with distinguishable surface and interior in the vicinity of a critical point.[8]

Another problem we need to face is the nature of the metastable state itself. In mean - field theories the free energy and equations of state in the metastable state are analytic continuations of their stable state counterparts. Is this still true for systems with finite range forces. If not, how do we describe the metastable state?

For all of the reasons discussed above we need to reexamine the theory of metastability and nucleation. In the next few lessons we will return to this problem with various techniques and examine some of the complications and subtleties.

3.2 Becker - Döring Theory

In order to understand the problem with the simple approach in lesson 1 we need to return to the beginning and reformulate it in more precise terms. This was done by Becker

and Döring in 1935.[9] The Becker - Döring theory is not without its own assumptions but it is a more fundemental theory than presented in lesson 1.

The basic assumption of the theory is that clusters with l monomers grow and decay via an evaporation - condensation mechanism where the droplet or cluster gains or loses a single molecule. Consequently the theory neglects coalesence and fission. The time derivative of the number of clusters of size l, $n_l(t)$ can be written as

$$\frac{\partial n_l(t)}{\partial t} = J_{l-1} - J_l \tag{3.2}$$

where

$$J_{l-1} - J_l = [R_{l-1}n_{l-1}(t) - R'_l n_l(t)] - [R_l n_l - R'_{l+1}n_{l+1}] \tag{3.3}$$

is the rate per unit volume at which droplets of size l are created. The term $R_{l-1}n_{l-1}$ is the rate per unit volume at which droplets with $l-1$ monomers gain a monomer to become droplets with l monomers and $R'_l n_l$ is the rate at which droplets with l monomers lose a monomer to become droplets with $l-1$ monomers. The second assumption of Becker - Döring is embodied in eq. 3.3. Namely that the rates of gain or loss of monomers from droplets of size l is proportional to n_l.

We can relate R and R' with another assumption. The assumption is that the system is very close to metastable **equilibrium**. What is meant by "very close" will be defined shortly. At equilibrium, either stable or metastable, the number of droplets or clusters of size l is given by equilibrium fluctuation theory. Namely

$$\bar{n}_l = \exp\left\{\frac{-\Delta F_l}{K_B T}\right\} \tag{3.4}$$

where ΔF_l is the free energy cost of a cluster of size l. At equilibrium the number of droplets of size l is a constant so that the time derivative of $n_l(t) = 0$. This implies

$$R_{l-1}\exp\left\{\frac{-\Delta F_{l-1}}{K_B T}\right\} = R'_l \exp\left\{\frac{-\Delta F_l}{K_B T}\right\} \tag{3.5}$$

Equation 3.5 relates R_{l-1} to R'_l but we still must determine R_l and justify the equilibrium assumption used to obtain eq. 3.5. Before doing these two things we will make the approximation that l can be treated as a continuous variable. The justification for this assumption is twofold. First the droplets only change by increasing or decreasing l by 1 and for all droplets of interest $l >> 1$. Having said that we point out that we will consider droplets with small l but that extension will not change the conclusions in any substantative way. We can now write

$$\frac{\partial n_l(t)}{\partial t} = -\frac{J_l - J_{l-1}}{\Delta l} = -\frac{\partial J_l}{\partial l} \tag{3.6}$$

where $\Delta l = 1$ is treated as an infinitesimal and J_l is given in the second bracket on the right hand side of eq. 3.3.

From eqs. 3.3 and 3.5 we have

$$+J_l = R_l n_l(t) - R_l \exp\left\{-\Delta \frac{F_l - \Delta F_{l+1}}{K_B T}\right\} n_{l+1}(t) \tag{3.7}$$

Expanding the exponential to first order we obtain

$$+J_l = R_l[n_l(t) - n_{l+1}(t)] + \frac{R_l}{K_B T}[\Delta F_l - \Delta F_{l+1}] n_l(t) \tag{3.8}$$

where we have set $n_{l+1}(t) = n_l(t) + \Delta n_l$ equal to n_l. Again treating $\Delta l = 1$ as an infinitesimal and using eq. 3.6 we obtain

$$\frac{\partial n_l(t)}{\partial t} = \frac{\partial}{\partial l}\left[\frac{R_l}{K_B T}\frac{\partial \Delta F_l}{\partial l} n_l(t) + R_l \frac{\partial n_l(t)}{\partial l}\right] \tag{3.9}$$

Returning to the question of determining R_l. We will again make the assumption that the droplets of interest are compact. That is

$$R_l \propto l^{(d-1)/d} \tag{3.10}$$

This is, of course, a classical assumption and we should not necessarily expect it to hold near critical points or spinodals where the vanishing of the surface tension could lead to a different expression.

We now address the question of what it means to be very close to equilibrium. Note that $\bar{n}_l$ as defined in eq. 3.4 is a solution to eq. 3.9. More over from eqs. 3.6 and 3.9 $n_l(t) = \bar{n}_l$ leads to the vanishing of J_l. A moments reflection leads to the conclusion that this is not the solution we are looking for. We don't want $J_l = 0$ which would imply that there is no "flow" of droplets from small l to large. We want to describe the situation where there is a very small flow. If the flow is too large then the density will be high enough so that there will be interaction of droplets. Moreover, the background would not be in metastable equilibrium.

The way around this dilema is to realize that if the lifetime of the metastable state is large, so that the density of critical droplets is small, then there will be a time interval during which droplets will go critical at a constant rate yet their number is so small that the effect on the background is neglegible. We use this idea to define a steady state condition. We postulate the existence of a steady state solution n_l^s such that $\frac{\partial n_l^s(t)}{\partial t} = 0$ but $J_l = I \neq 0$ where I is a constant. We impose this condition by requiring

$$\lim_{l \to 0} n_l^s = \bar{n}_l \; and \; \lim_{l \to \infty} n_l^s = 0 \tag{3.11}$$

These boundary conditions, usually referred to as the source and sink conditions, can be viewed physically as taking droplets that grow beyond some critical size, breaking them up, and returning them to the background to keep $n_l(t) \sim \bar{n}_l$ for small l.

The solution of eq. 3.9 that satisfies these conditions is

$$n_l^s = I \int_l^\infty \frac{\bar{n}_l}{R_{l'}\bar{n}_{l'}} dl' \tag{3.12}$$

and

$$I^{-1} = \int_0^\infty \frac{dl}{R_l \bar{n}_l} \tag{3.13}$$

as can be seen by substitution. The form of $\bar{n}_l$ is given in eq. 3.4

Let us consider the Ising model where

$$\Delta F_l = hl + \sigma l^{\frac{d-1}{d}} \tag{3.14}$$

From eqs. 3.4, 3.10, 3.13 and 3.14 the inverse of the nucleation rate is

$$I^{-1} = \int_0^\infty \frac{\exp\left[-|h|l + \sigma l^{\frac{d-1}{d}}\right]}{l^{\frac{d-1}{d}}} dl \tag{3.15}$$

where the magnetic field h is negative since we are in the metastable state. We now define the variable

$$t \equiv \frac{|h|^d}{\sigma^d} l \tag{3.16}$$

With eq. 3.16, eq. 3.15 becomes

$$I^{-1} = \frac{\sigma}{|h|} \int_0^\infty \frac{\exp\left[-\frac{1}{K_B T} \frac{\sigma^d}{|h|^{d-1}} (t - t^{\frac{d-1}{d}})\right]}{l^{\frac{d-1}{d}}} dt \tag{3.17}$$

Near the coexistence curve i. e. $h \sim 0$ the integral in eq. 3.17 can be done with the methods of steepest descent. We obtain

$$I = \frac{|h|}{\sigma} \left[\frac{d-1}{d}\right]^{d-1} \left\{\frac{\sigma^d (d-1)}{d^2 K_B T |h|^{d-1}}\right\}^{\frac{1}{2}} \exp\left[-\frac{\sigma^d (d-1)^{d-1}}{K_B T |h|^{d-1} d^d}\right] \tag{3.18}$$

Note that the saddle point value of $l \propto (\sigma/|h|)^d$ is the droplet critical radius of lesson 1 raised to the power d.

Equation 3.18 should be compared with the expression for τ^{-1} where τ is given in eq. 1.13. Note that the exponential terms are the same but in eq. 3.18 we have also obtained an expression for the prefactor to the exponential. We have also made precise someting that was glossed over in lesson 1, namely that the nucleation rates we are considering in

both lessons are steady state rates. However there are still problems. For example the dependence on the conservation laws is not clear. We started with eq. 3.2 which has no order parameter conservation and it is at this point not clear how to put it in if it is needed. A second point is that the structure of the droplet is not obtained from this theory. At best it is put in by hand in eq. 3.10. For these reasons we are looking for something better than Becker - Döring theory. To facilitate the development of a better theory we next look at the so called classical droplet model.

3.3 Classical Droplet Model

In this section we will consider a system at low temperature which will consist of a uniform background of spins and excitations or fluctuations consisting of compact objects which are presumed to be rare enough that their interactions can be neglected. These fluctuations or droplets do however interact with the background and an applied external field. The energy of to create one of these excitations with l monomers is

$$H = hl + Jl^{\frac{d-1}{d}} \tag{3.19}$$

where h is the magnetic field and J is proportional to the spin - spin interaction. The first term in eq. 3.19 is the interaction with the field and the second term is the interaction with the background. We want to calculate the free energy in the grand canonical ensemble. First consider the case for a fixed size l of the droplets. The chemical potential μ is defined as $\frac{\partial E}{\partial n}$ where E is the total energy of interaction of the droplets of size l with the field and background.[10] Since the droplets are assumed to be non interacting the energy for n droplets of size l is given by

$$E_l = \left[hl + Jl^{\frac{d-1}{d}}\right]n \tag{3.20}$$

Hence the chemical potential for droplets of size l is

$$\mu_l = hl + Jl^{\frac{d-1}{d}} \tag{3.21}$$

The activity z_l is defined as

$$z_l \equiv \exp(-\beta\mu_l) \tag{3.22}$$

We can now calculate the grand canonical partition function Ξ_l for droplets of size l.

$$\Xi_l = \sum_n \frac{z_l^n}{n!} Q_{nl} \tag{3.23}$$

The term Q_{nl} is the cononical partition function of a system of n non interacting droplets of size l and hence equal to V^n where V is the volume of the system.

From eqs. 3.21 - 3.24 we obtain

$$\begin{aligned}\Xi_l &= \sum_n \frac{V^n}{n!} \exp\{-\beta(hl + Jl^{\frac{d-1}{d}})n\} \\ &= \exp\{\exp[-\beta(hl + Jl^{\frac{d-1}{d}}]V\}\end{aligned} \tag{3.25}$$

The Gibbs free energy per unit volume for clusters of size l is

$$\frac{1}{V}\ln \Xi_l = \exp\left[-\beta(hl + Jl^{\frac{d-1}{d}}\right] \tag{3.26}$$

Since the droplets are non - interacting we can obtain the free energy per unit volume, $f(h, J)$, by summing over all droplet sizes.

$$f(h, J) = \sum_l \exp\left[-\beta(hl + Jl^{\frac{d-1}{d}})\right] \tag{3.27}$$

This is the free energy for the classical droplet model; classical because it assumes compact droplets. This should be a good assumption if we are not near any critical points.

We now define a variable t' in the same way we defined t in eq. 3.16.

$$t' \equiv \frac{|h|^d}{J^d} l \tag{3.28}$$

and restrict our consideration to $|h| << 1$. In this limit t' can be considered a continuous variable and eq. 3.27 can be written as

$$f(h, J) = \frac{J^d}{|h|^d} \int_0^\infty \exp\left[-\frac{J^d}{|h|^{d-1}}(\alpha t' + t'^{\frac{d-1}{d}})\right] dt' \tag{3.29}$$

where α is the sign of h. For stable equilibrium $\alpha = 1$. We want to extent our model to study the metastable state. In the stable state the magnetic field term h produces an increase in the energy when a droplet is created. In the metastable state the magnetic field term produces a lowering of the energy when a droplet appears. This implies that $h < 0$ in the metastable state or that $\alpha = -1$ in eq. 3.29. Unfortunately for $\alpha = -1$ the sum in eq. 3.27 or the integral in eq. 3.29 will not converge. This makes sense physically since negative values of h should correspond to the "other" stable phase. However the equilibrium state corresponding to negative values of h requires a change in the background that this model in its present form cannot accomodate. However, this does not prevent the use of this model to describe the metastable state. Before discussing the formal aspects of this description let's take another look at eq. 3.27 for negative h.

The argument of the exponential in eq. 3.27 is

$$\beta\{|h|l - Jl^{\frac{d-1}{d}}\} \tag{3.30}$$

where we have taken $h < 0$. The sum over droplet size l will cause the argument in eq. 3.30 to decrease (become more negative) until $l = l_c$ where

$$l_c = \left[\frac{d-1}{d}\right]^d \left\{\frac{J}{|h|}\right\}^d \tag{3.31}$$

The term l_c is very reminicient of the critical size in the theory of nucleation in lesson 1. Until $l = l_c$ the partition function sum in eq. 3.27 has the properties of an equilibrium quantity. This is in fact one way to describe metastability in the droplet model contex; namely restricting the sum over l to $l < l_c$ and l_c defines the critical droplet.

There are however, several questions that need to be considered. First, the restriction to $l < l_c$ is not unique. Why not truncate the sum at $2l_c$ or $\frac{1}{2}l_c$? This is a valid question and one that corresponds to a real physical ambiguity. There is a certain randomness to nucleation and although a droplet may exceed the critical length l_c and should grow fluctuations may drive it back. The second question we must address if we are to use the idea of a truncated sum is; How do we relate the critical size l_c at which we truncate the partition function sum to the nucleation rate? Finally; How do we account for the dependence of the nucleation rate on temperature and dynamics seen in figs. 3.1 - 3.3.

Following Langer[11] we will take a different route to the metastable state which will make the connection between the critical droplet and the nucleation rate. Rather than setting $\alpha = -1$ in eq. 3.29 suppose we analytically continued α from 1 to -1. We can keep the modulus of $\alpha = 1$ so we can set $\alpha = e^{i\theta}$. Although the integration can be done in the variables of eq. 3.29 it will be more transparent if we define $z^d \equiv t'$. Equation 3.29 becomes

$$f(h,J) = \frac{dJ^d}{|h|^{d-1}} \int_0^\infty z^{d-1} \exp\left[-\frac{J^d}{|h|^{d-1}}(\alpha z^d + z^{d-1})\right] dz \tag{3.32}$$

In order to analytically continue $f(h,J)$ to negative h we set $z = \rho e^{i\phi}$. The integral in eq. 3.32 will always be done on a contour in the complex z plane such that the real part of αz^d is positive. In that way we will guarantee the convergence of the integral. This restriction implies that $\cos(\theta + d\phi) > 0$. Consider the integral over the contour in fig. 3.4. From the Cauchy theorem the integral equals zero. Assume that $\theta = 0$. If ϕ is chosen such that $\cos(d\phi) > 0$ then the contribution over the semi - circular part of the contour will vanish as $s \to \infty$. Therefore the integral from A to B equals the integral from A to C.

However the integral from A to C converges over a different range of θ than the integral from A to B.

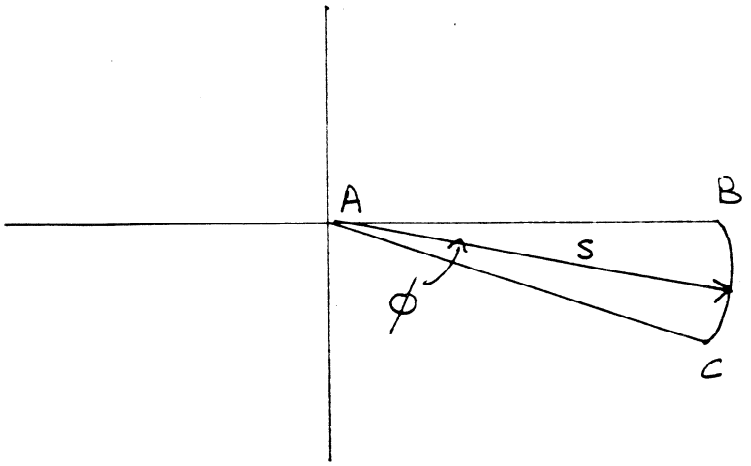

Fig. 3.4 Contour used to analytically continue $f(h, J)$.

For example, suppose $d = 2$ and $\phi = \pi/8$. Then for $\theta = 0$ the contribution over the semi - circular contour from B to C vanishes since the exponential in the integrand of eq. 3.32 equals

$$\exp\left[-\frac{J^d}{|h|^{d-1}}\{\cos(2\phi)s^2 + s\}\right] \tag{3.33}$$

and ϕ varies between 0 and $\pi/8$. Moreover the integral over the part of the contour between C and A also converges since $\cos(\pi/4) > 0$. However the integral over the A to C segment will converge for values of $\theta > 0$. We need only require that $\cos(\theta + \pi/4) > 0$ or $-\pi/2 < \theta + \pi/4 < \pi/2$. Therefore the integral over A to C converges for $-3\pi/4 < \theta < \pi/4$. Note that the integral over A to C will converge for $\theta = 0$ but will also converge for values of θ for which the integral over A to B will not. The integral over A to C is the analytic continuation of the integral over A to B. We can continue this process until $\theta = \pi$ and in this way analytically continue to $\alpha = -1$.

We could have also analytically continued by rotating θ to $-\pi$ which would have necessitated rotating the **contour** clockwise rather than the counter clockwise rotation depicted in fig. 3.4. Note that for $\theta = \pi$ the range of ϕ is from $-3\pi/4$ to $-\pi/4$ in $d = 2$. For $\theta = -\pi$, ϕ ranges from $\pi/4$ to $3\pi/4$. The fact that these two ranges for ϕ do not overlap indicates that there is a branch point at $h = 0$ and we have put the branch cut on the negative real axis. There are two distict contours. One describes the rotation $\theta \to \pi_+$ and the other $\theta \to \pi_-$ For $\alpha = -1$ all terms in the integrand in eq. 3. are real except of course z. We can chose our two seperate contours for the two different approaches to $\alpha = -1$ to be symmetric about the real axis. Therefore $f(|h|, J, \alpha \to -1_+)$ is the complex conjugate of $f(|h|, J, \alpha \to -1_-)$

As we discussed above we are working in the limit $h \sim 0$. Consequently the integral in eq. 3.32 can be done with the method of steepest descent. [12]. From eq. 3.32 the saddle point is at

$$z_c = -\frac{d-1}{\alpha d} \tag{3.34}$$

As α is rotated, the saddle point rotates in the complex z plane until for $\alpha = -1$ the saddle point is at $z_c = \frac{d-1}{d}$. In order to do the integrals corresponding to the analytic continuation we use the contours shown in fig. 3.5

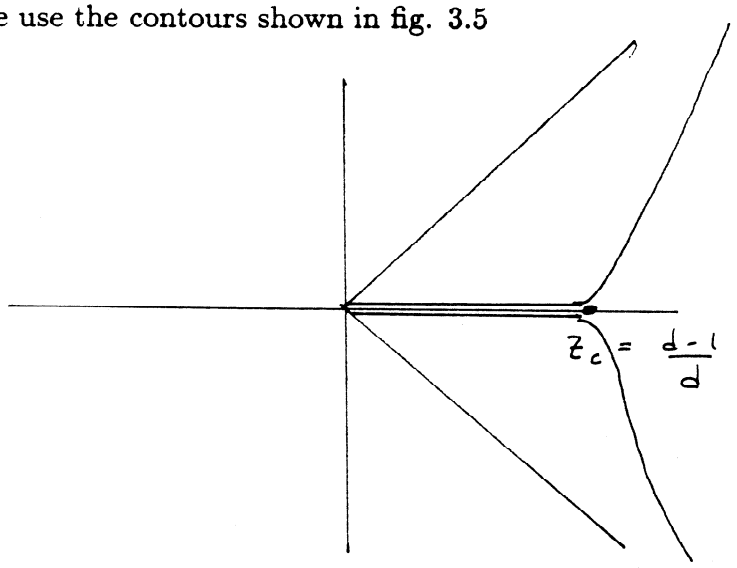

Fig. 3.5 Steepest descent contours for analytic continuation.

The contours shown in fig. 3.5 start at the origin, run along the real axis up to the saddle point, go down the path of steepest descent and asymptotically approach the lines drawn at $\phi = \pi/4 + \epsilon$ and $\phi = -\pi/4 - \epsilon$. Since two contours give free energies which are complex conjugates of each other the real parts are the same. The difference in the two free energies $f(|h|, J, \alpha \rightarrow -1_+) - f(|h|, J, \alpha \rightarrow -1_-)$ is twice the imaginary part and is evaluated over the contour shown in fig. 3.6. This countour is the difference of the two contours in fig. 3.5.

It makes sense to consider the integral from the origin to the saddle point along the real axis in fig. 3.5 as the metastable state free energy. The saddle point value of z corresponds to the critical droplet value of $l = l_c$ hence the integral along the real axis up to z_c will correspond to the restricted partition function sum discussed above.

What is the physical significance of the imaginary part of the free energy? Evaluating the integral in eq. 3.32 over the contour shown in fig. 3.6 using steepest descent[12] yields

$$2Imf(|h|, J, \alpha \to -1_+) = M\frac{dJ^d}{|h|^{d-1}}\left[\frac{d-1}{d}\right]^{d-1}\exp\left\{-\frac{J^d}{K_BT|h|^{d-1}}\frac{(d-1)^{d-1}}{d^d}\right\} \quad (3.35)$$

where

$$M = \left[\frac{J^d\pi(d-1)^{d-1}}{K_BT|h|^{d-1}d^{d-2}}\right]^{-\frac{1}{2}} \quad (3.36)$$

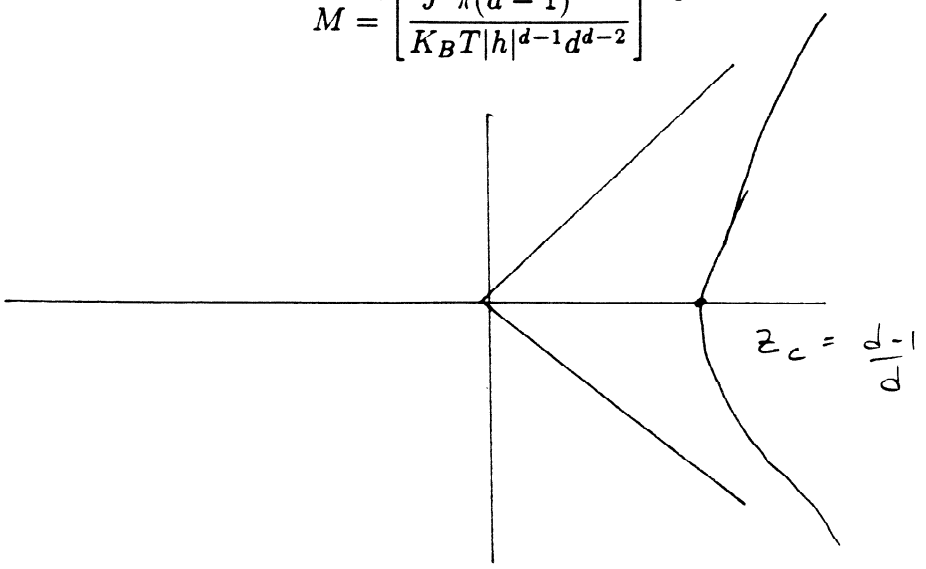

Fig. 3.6 Contour for the imaginary part of the free energy in eq. 3.35

We can now compare eqs. 3.35 and 3.36 with 3.18 obtained from the Becker - Döring theory. The first thing to notice is that the exponential terms in eqs. 3.18 and 3.35 are the same. That is the free energy cost of the critical droplet from the analytic continuation, Becker - Döring and the simple theory in lesson one are dominated by the same exponential term. The second point is that the prefactor in eq. 3.35, which includes the constant M in eq. 3.36 is different than the prefactor in eq. 3.18. Of course we are not referring to the replacement of σ in 3.18 by J in 3.35. The surface tension $\sigma \sim J$ for $T << T_c$ where we expect the classical droplet model to be accurate. We are referring to the different dependence on $|h|$ and J. From the discussion in the introduction we might assume that the difference is due to the inclusion in the Becker - Döring theory,of dynamic effects not included in the purely static analytic continuation. The similarity is however striking. This led Langer[11] to conclude that at least a part of nucleation rate could be obtained from the analytic continuation of the free energy. This is in many ways reminicient of the relation between the lifetime of a resonance and the imaginary part of the scattering amplitude.[13] We will also persue this point of view using the droplet model as a paradigm. When we translate these ideas into the language of scalar field theory we obtain the most powerful technique presently available to describe the nucleation process.

References Lesson 3

1. see ref. 7, lesson 1
2. T. S. Ray and J. S. Wang (to be published)
3. R. Swendsen and J. S. Wang, Phys. Rev. Lett. **58**, 86 (1987)
4. see ref. 3, lesson 2
5. D. W. Heermann, W. Klein and D. Stauffer, Phys. Rev. Lett. **47**, 1262 (1982)
6. C. Domb and N. W. Dalton, Proc. Phys. Soc. **89**, 859 (1966)
7. W. Klein and C. Unger, Phys. Rev. **B28**, 445 (1983)
8. A. Coniglio and W. Klein, J. Phys. **A13**, 2775 (1980)
9. see ref. 2, lesson 1
10. see ref. 1, lesson 1
11. J. S. Langer, Annals of Physics **41**, 108 (1967)
12. *Mathematical Methods of Physics*, J. Mathews and R. L. Walker (Benjamin, New York 1965)
13. *Quantum Mechanics Volume 1: Fundementals* K. Gottfried (Benjamin, New York, 1966)

Lesson 4

4.1 Introduction

In this lesson we will follow the paradigm discussed in Lessons 1 and 3. Namely, we will use the Landau - Ginsburg free energy as a Hamiltonian or action. This approach is well known in field theory and critical phenomena[1,2] and it is one of the most powerful tools known for describing phase transitions. Although these methods are useful for several classes of systems such as x-y and Heisenberg models, super conductivity and fluidity and percolation we will, at least for now, restrict our considerations to Ising, binary and fluid systems. For the processes we wish to study these are pretty much the only systems for which clean data, both numerical and real, exists.

If you are interested in the details of how one converts from a Landau - Ginsburg free energy to a Landau - Ginsburg - Wilson Hamiltonian please consult reference 1 or 2 or ref. 11 in Lesson 3.

Our point of departure will be the partition function

$$z = \int \delta\phi \exp\{-\beta H(\phi)\} \tag{4.1}$$

where

$$-\beta H(\phi) = -\beta \int [\frac{R^2}{2}(\nabla\phi(\vec{x}))^2 + \epsilon\phi^2(\vec{x}) + \phi^4(\vec{x}) - h\phi(\vec{x})]\, d\vec{x} \tag{4.2}$$

Equation 4.2 is the same as eq. 1.7 except that now we are using it as a Hamiltonian rather than a free energy. The integral in eq. 4.1 is a functional integral over all functions $\phi(\vec{x})$. We define a new variable $\vec{r} = \vec{x}/R$ so that eq. 4.2 becomes

$$-\beta H(\phi) = -\beta R^d \int [\frac{1}{2}(\nabla\phi(\vec{r}))^2 + \epsilon\phi^2(\vec{r}) + \phi^4(\vec{r}) - h\phi(\vec{r})]\, d\vec{r} \tag{4.3}$$

The partition function becomes

$$z = \int \delta\phi \exp[-\beta R^d H(\phi)] \tag{4.4}$$

If β or R is large then the partition function can be approximated quite well using steepest descent techniques. We will assume that we are working in this limit. Therefore we will take either $R >> 1$ or $T << T_c$ or both.

4.2 Saddle Points and Gaussian Fluctuations

To evaluate the steepest descent integral we first find the saddle points. In order to find the saddle points we functionally differentiate the argument of the exponential in eq. 4.4, i. e. the Hamiltonian in eq. 4.3.

To evaluate the derivative of a functional $H(\phi)$ we consider the functional $H(\phi(\vec{r}) + \eta(\vec{r}))$ where η is a small perturbation. We then write

$$H(\phi + \eta) \approx H(\phi) + \int H'(\phi)\eta(\vec{r})d\vec{r} \tag{4.5}$$

This expression defines the functional derivative $H'(\phi)$. From eq. 4.3

$$H(\phi+\eta) = R^d \int [\frac{1}{2}(\nabla(\phi(\vec{r})+\eta(\vec{r}))^2 + \epsilon(\phi(\vec{r})+\eta(\vec{r}))^2 + (\phi(\vec{r})+\eta(\vec{r}))^4 - h(\phi(\vec{r})+\eta(\vec{r}))]d\vec{r} \tag{4.6}$$

Expanding the righthand side of eq. 4.6 and keeping only up to linear terms we obtain

$$H(\phi + \eta) \approx H(\phi) + R^d \int [\nabla\phi(\vec{r})\nabla\eta(\vec{r}) + 2\epsilon\phi(\vec{r})\eta(\vec{r}) + 4\phi^3(\vec{r})\eta(\vec{r}) - h\eta(\vec{r})]d\vec{r} \tag{4.7}$$

The term $\int \nabla\phi(\vec{r})\nabla\eta(\vec{r})d\vec{r}$ is not quite in the right form. To get it in the proper form we integrate by parts using the boundary conditions that $\eta(\vec{r}) \to 0$ as $|\vec{r}| \to \infty$ to obtain

$$H(\phi + \eta) \approx H(\phi) + R^d \int [-\nabla^2\phi(\vec{r}) + 2\epsilon\phi(\vec{r}) + 4\phi^3(\vec{r}) - h]\eta(\vec{r})d\vec{r} \tag{4.8}$$

The saddle point is the solution of

$$-\nabla^2\phi(\vec{r}) + 2\epsilon\phi(\vec{r}) + 4\phi^3(\vec{r}) - h = 0 \tag{4.9}$$

We first consider the solutions of eq. 4.9 that are spatial constants. Assuming $\phi(\vec{r}) = \phi =$ constant eq. 4.9 becomes

$$2\epsilon\phi + 4\phi^3 - h = 0 \tag{4.10}$$

For $\epsilon > 0$ there is one real solution to eq. 4.10. For $\epsilon < 0$ there are three real solutions, one maximum and two minima. This is strongly reminicient of the discussion in lesson 1 following eq. 1.9, and with good reason. As βR^d becomes large so that we can use the saddle point technique the system is becoming more mean-field. This is illustrated in fig. 3.3 for the susceptibility.

Let's look more closely at z for $\epsilon > 0, h = 0$. To complete the steepest descent evaluation of the partition function we must evaluate the Gaussian integral about the saddle point. In order to do this we first need the second functional derivative of the functional $H(\phi)$ and the functional Taylor series expansion up to second order. To obtain these quantities we return to eq. 4.5. The term $\int H'(\phi)\eta(\vec{r})d\vec{r}$ is first order in the small parameter $\eta(\vec{r})$. In order to have an equality rather than the approximate equality in eq. 4.5 we should write

$$H(\phi + \eta) = H(\phi) + \int H'(\phi + \eta)\eta(\vec{r})d\vec{r} \tag{4.11}$$

We can now expand H' to first order in $\eta(\vec{r})$ to obtain

$$H(\phi+\eta) \approx H(\phi) + \int H'\eta(\vec{r})d\vec{r} + \int H''(\phi)\eta(\vec{r})\eta(\vec{r}')d\vec{r}d\vec{r}' \tag{4.12}$$

where we have kept terms up to second order in η.

An equivalent, and perhaps easier way to obtain the functional derivative is to use a variable ω in the argument of the functional $H(\phi)$. We can then define the functional derivative through the realtion[3]

$$\frac{d}{d\omega}H(\phi(\vec{r}) + \omega\eta(\vec{r})) = \int H'(\phi(\vec{r}))\eta(\vec{r})d\vec{r} \tag{4.13}$$

The functional Taylor series can simply be seen in eq. 4.12 up to second order. In fact it is the functional Taylor series that is used to define the derivative. With these considerations we return to eq. 4.6, expand and keep terms up to second order. We obtain

$$H(\phi) \approx H(\phi_o) + \int \left[-\eta(\vec{r})\nabla^2\eta(\vec{r}) + 2\epsilon\eta^2(\vec{r}) + 12\phi_o^2\eta^2(\vec{r})\right]d\vec{r} \tag{4.14}$$

where ϕ_o is the solution to eq. 4.10.

The partion function integral in eq. 4.4 reduces to

$$z \approx \exp\left[-\beta R^d H(\phi_o)\right] \int \delta\eta \exp\left[-\beta R^d \int \left\{-\eta(\vec{r})\nabla^2\eta(\vec{r}) + 2\epsilon\eta^2(\vec{r}) + 12\phi_o^2\eta^2(\vec{r})\right\}d\vec{r}\right] \tag{4.15}$$

To do the functional Gaussian integral we want to diagonalize the Gaussian form in eq. 4.15. Specifically we write

$$-\eta(\vec{r})\nabla^2\eta(\vec{r}) + 2\epsilon\eta^2(\vec{r}) + 12\phi_o^2\eta^2(\vec{r}) = \eta(\vec{r})\left[-\nabla^2\eta(\vec{r}) + 2\epsilon\eta(\vec{r}) + 12\phi_o^2\eta(\vec{r})\right] \tag{4.16}$$

Returning to the $\epsilon > 0, h = 0$ case and writing

$$\eta(\vec{r}) = \int \exp\left[i\vec{k}\cdot\vec{r}\right]\hat{\eta}(\vec{k})d\vec{k} \tag{4.17}$$

the right hand side of eq. 4.16 becomes

$$\int\int\int e^{-i\vec{k}'\cdot\vec{r}}e^{i\vec{k}\cdot\vec{r}}\left[|\vec{k}|^2 + \epsilon\right]\hat{\eta}^*(\vec{k}')\hat{\eta}(\vec{k})d\vec{r}d\vec{k}d\vec{k}' = \int\left[k^2 + \epsilon\right]|\hat{\eta}(\vec{k})|^2 d\vec{k} \tag{4.18}$$

where we have used $k = |\vec{k}|$ and

$$\eta(\vec{r}) = \eta^*(\vec{r}) = \int e^{-i\vec{k}'\cdot\vec{r}}\hat{\eta}^*(\vec{k}')d\vec{k}' \tag{4.19}$$

and the $\vec{r}$ integration produces a $\delta(\vec{k}-\vec{k}')$.

The functional integral in eq. 4.15 can now be written as

$$\int \delta\hat{\eta}(\vec{k}) \exp\left[-\beta R^d \int (k^2+\epsilon)|\hat{\eta}(\vec{k})|^2 d\vec{k}\right] \tag{4.20}$$

Since we expect radial symmetry we can take $\eta(\vec{r}) = \eta(|\vec{r}|)$. This in turn implies that $|\eta(\vec{k})|^2 = \eta^2(k)$. Also note that we have written the functional integral with respect to $\eta(\vec{r})$ as an integral over the Fourier coefficients $\hat{\eta}(\vec{k})$. This allows us to do the integral in eq. 4.20 as a product of Gaussian integrals in the scalar variables $\hat{\eta}(\vec{k})$ for each value of $\vec{k}$. In a sense the evaluation of the functional Gaussian integral is similar to the way the propagator is evaluated in a Feynman path integral representation of the quadratic Lagrangian.[4]

The partition function in eq. 4.15 can now be written as

$$z \approx exp\left[-\beta R^d H(\phi_o = 0)\right] \prod_{\vec{k}} \left\{\frac{\pi}{(k^2+\epsilon)}\right\}^{1/2} \tag{4.21}$$

and the free energy as

$$F = -K_B T \ln z \approx \frac{1}{2} K_B T \int d\vec{k} \ln\left[(k^2+\epsilon)\pi^{-1}\right] \tag{4.22}$$

At this point we briefly digress to ask how we can actually write the integral in eq. 4.15 as the product of simple Gaussian integrals. The problem specifically is how we deal with the continuum of $\vec{k}$ values. The answer lies in doing the calculation in a finite volume L^d and in the end taking the limit $L \to \infty$. For finite L we do not have a continuum of eigenvalues for the free particle Schrödinger operator in eq. 4.16, we have a discreet set with a density proportional to L^{-d}. This is, of course, the spectrum of a free particle in a box in Quantum Mechanics. We now have a sum over discreet values of $\vec{k}$ rather than an integral over the $\vec{k}$ continuum in eq. 4.20. The details of this proceedure are given in ref. 1 chapter 2 and we will not go into them here. The upshot is that the expression for the free energy in eq. 4.22 is modified by multiplication by the factor L^d. The critical exponent α can be calculated from the free energy[1] in eq. 4.22 and we refer the interested reader to ref. 1. The relevant point for our purposes is that it is the small amplitude modes, which can be treated in the Gaussian approximation, that are responsible for the part of the equilibrium free energy due to fluctuations. Of course this is only in the $R \to \infty$ or $T \to 0$ limit. Note also that the system is stable to these modes or fluctuations and this can be seen from the positivity of the eigenvalues of the Schrödinger operator in eq. 4.16 i. e.

$$\lambda_k = k^2 + \epsilon \tag{4.23}$$

For $\epsilon < 0$ there are three solutions to eq. 4.10. As we saw in Lesson 1 two are minima and one is a maximum. When $h = 0$ the two minima are of equal depth but when $h \neq 0$ one minimum is lower than the other. Concentrating now on the $\epsilon < 0$ case we take, for example $h > 0$ initially. If we perform the functional integral for the partition function in eq. 4.4 with the steepest descent technique we will obtain the dominant contribution from the saddle point at $\phi = \phi_{o+}$, where ϕ_{o+} is the solution of eq. 4.10 for $h > 0$ and $\epsilon < 0$ that corresponds to the absolute minimum. What about the small amplitude Gaussian fluctuations? The same proceedure we used for $\epsilon > 0, h = 0$ can be used in the vicinity of the ϕ_{o+} saddle point but now the einenvalues λ_k are given by

$$\lambda_k = k^2 - 2|\epsilon| + 12\phi_{o+}^2 \tag{4.24}$$

The positivity of λ_k in eq. 4.24 is guaranteed by the fact we are in the stable state. In other words $\lambda_k > 0$ because we are restricting ourselves to considering only those values of h and ϵ for which the inequality holds. We considered those regions for which the inequality did not hold in Lesson 2.

4.3 Metastable States

We now want to consider $h < 0$. If we simply set h equal to some negative value we expect, by symmetry, that the same considerations as above still apply except we would evaluate the partition function around the ϕ_{o-} saddle point. To some extent this is remincient of the droplet model in Lessson 3. In that case we could not set the magnetic field equal to a negative value and obtain another phase because the model was not rich enough. However, we could reach the metastable phase by analytic continuation.

We will follow the same proceedure here. That is, we will analytically continue the free energy to negative values of h. To see what is happening consider the simple model obtained from eq. 4.4 for the partition function by restricting the variable $\phi(\vec{r})$ to a constant ϕ. The partition function integral in this model will be

$$\tilde{z} = \int d\phi \exp\left[-\beta R^d(-|\epsilon|\phi^2 + \phi^4 - h\phi)\right] \tag{4.25}$$

There are now two saddle points of interest; the two minima. The deeper minimum will dominate the saddle point integral so that in the limit $R \to \infty$ the stable state will always dominate the partition function sum as expected. Suppose we now expand the argument of the exponential in eq. 4.25 about the saddle point ϕ_{o+} with $h > 0$. We can also refer to this saddle point as the positive magnitization saddle point. Clearly in

equilibrium for $h > 0$ $\phi_{o+} > 0$. Expansion about this saddle point gives

$$
\begin{aligned}
&-|\epsilon|\phi^2 + \phi^4 - h\phi = \\
&-|\epsilon|\phi_{o+}^2 + \phi_{o+}^4 - h\phi_{o+} + \frac{f''(\phi_{o+})}{2}(\phi - \phi_{o+})^2 + 2\phi_{o+}(\phi - \phi_{o+})^3 + (\phi - \phi_{o+})^4
\end{aligned}
\tag{4.26}
$$

where $f''(\phi_{o+})$ is the second derivative of the left hand side of eq. 4.26 evaluated at $\phi = \phi_{o+}$. Focus your attention on the cubic term. If we are close to the saddle point then the quadratic term dominates. If we increase $-(\phi - \phi_{o+})-$ then the cubic term will eventually dominate the quadratic for $\phi - \phi_{o+} < 0$ and the presence of the other saddle point will be felt. If $h > 0$ so that ϕ_{o+} is the stable state, it will not matter that another saddle point exists since ϕ_{o+} will dominate. However, suppose that we analytically continue to $h < 0$ The saddle point at ϕ_{o+} will move slightly to, say, ϕ'_{o+} but it will no longer be the dominant saddle point. The dominant saddle point will be at ϕ_{o-}. The cubic term in the expansion about ϕ'_{o+} will now indicate the presence of another, dominant saddle point. We can avoid the evaluation of the integral at the dominant saddle point, and hence obtain a description of the metastable state, by deforming the contour of integration in eq. 4.25 so that the cubic term remains positive. We will not do this here but simply note that the method is almost identical to the one used in Lesson 3 for the classical droplet model. We now want to evaluate the partition function in the neighborhood of the metastable saddle point having analytically continued as outlined above.

The small amplitude Gaussian fluctuations about the metastable saddle point ϕ'_{o+} for $h < 0$ can be handled in the same way we dealt with such fluctuations for $\epsilon > 0, h = 0$. The eigenvalues λ_k are given by

$$\lambda_k = k^2 - \epsilon + 12\phi_{o+}'^2 \tag{4.27}$$

As with the stable state saddle points and the eigenvalues in eq. 4.27 are positive. This positivity distinguishes the metastable from the unstable states discussed in Lesson 2 where the λ_k are negative for some range of k.

4.4 Nucleation - General Considerations

If the Gaussian fluctuations were the only ones, then the metastable state would, in fact, be stable. Some indication of what we might expect can be obtained by recalling that the critical droplet initiating the metastable state decay was associated with a saddle point in the classical droplet model. What kind of saddle point would we need to describe a critical droplet? Clearly it must be a spatially non - constant solution of eq. 4.9. If we are looking for a solution of eq. 4.9 what boundary conditions should we employ? The

boundary conditions, as usual, must come from the physics. First, we expect a radially symmetric solution. This expectation arises from the symmetry of the differential equation. With this assumption eq. 4.9 becomes

$$-\frac{d^2\phi(r)}{dr^2} - \frac{(d-1)}{r}\frac{d\phi(r)}{dr} - 2|\epsilon|\phi(r) + 4\phi^3(r) - h = 0 \tag{4.28}$$

If $\phi(r)$, the solution of eq. 4.28, is to represent the critical droplet then for physical reasons we do not expect any kinks at $r = 0$. This physical condition implies the boundary condition

$$\frac{d\phi(r)}{dr}\Big]_{r=0} = 0 \tag{4.29}$$

The second boundary condition arises from the expectation that the critical droplets are localized in space. Specifically, as $r \to \infty$ we expect the order parameter (i. e. $\phi(r)$) to approach the value of the metastable state background for large r. Note that the solution $\phi(r)$ to eq. 4.28 is not just the critical droplet, but the order parameter of a system that contains an isolated critical droplet as well as the uniform metastable state.

It is extremely difficult to obtain solutions to eq. 4.28. Non - linear differential equations are notoriously difficult to solve. Equation 4.28 has been solved numerically and we will look at these solutions shortly. However, it is possible to obtain a significant amount of insight into the physics by looking at two limits; $h \approx 0$ and deep quenches near the spinodal. We begin with $h \approx 0$.

4.5 Classical Nucleation

What can we learn about the solutions to eq. 4.28 for $h \approx 0$ without actually solving the equation? Following Langer[5] we can think of eq. as 4.28 as describing the motion of a particle in a displacement dependent potential. Noting that the force is the **negative** gradient of the potential, we rewrite eq. 4.28 as

$$\frac{d^2\phi(r)}{dr^2} = -\frac{(d-1)}{r}\frac{d\phi(r)}{dr} - 2|\epsilon|\phi(r) + 4\phi^3(r) - h \tag{4.30}$$

If we think of $\phi(r)$ as a time dependent displacement $x(t)$ and r as the time t we have

$$\frac{d^2x(t)}{dt^2} = -\frac{(d-1)}{t}\frac{dx(t)}{dt} - 2|\epsilon|x(t) + 4x^3(t) - h \tag{4.31}$$

The left hand side of eq. 4.31 is mass times acceleration (mass = 1). The right hand side consists of a time dependent friction force,

$$-\frac{(d-1)}{t}\frac{dx(t)}{dt} \tag{4.32}$$

and a displacement dependent force

$$-2|\epsilon|x(t) + 4x^3(t) - h \tag{4.33}$$

The potential associated with this force, $V(x)$, is plotted in fig. 4.1.

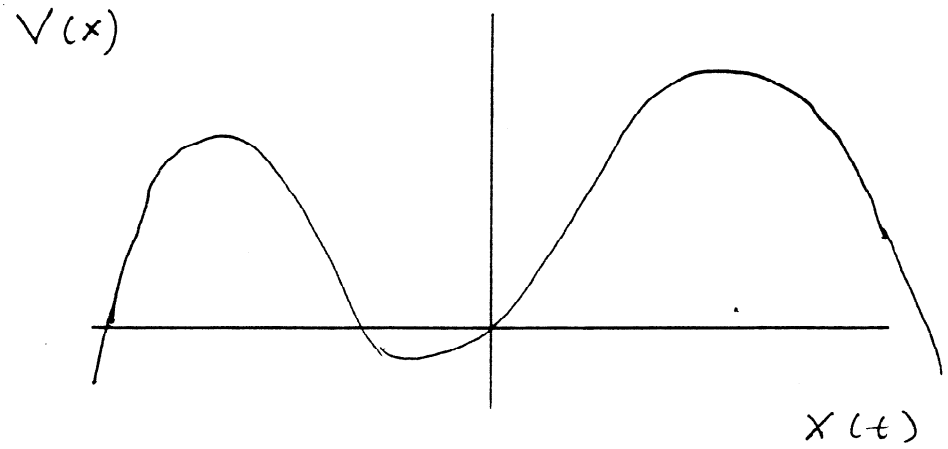

Fig. 4.1 $V(x)$ as a function of $x(t)$ for $h \approx 0$. The hill on the left is lower than the hill on the right.

The potential is the inverse of the free energy since the force is the negative gradient of the potential. The time is the variable r so that the boundary condition that $\phi(r)$ goes over to the metastable order parameter as $r \to \infty$ translates into the particle comes to rest at the top of the smaller (metastable) hill in fig 4.1 as $t \to \infty$. The boundary condition that the derivative of $\phi(r)$ equals zero at $r = 0$ (eq. 4.29) translates to the condition that the initial velocity of the particle is zero. The motion we are looking for then is that the particle starts at rest near the top of the higher hill (stable state minimum), rolls down the larger hill and up the smaller one and comes to rest at the top of the smaller hill (metastable minimum).

As $h \to 0$ the heights of the two hills become equal. Since the friction force is non - conservative we must have that the effect of this non - conservative force will also go to zero as $h \to 0$. The only way this can happen is that the particle starts closer to the top of the bigger hill as $h \to 0$. This will make the initial acceleration smaller and keep the particle near the top of the larger hill for a longer time. Since the friction force in eq. 4.32 decays as t^{-1} the longer the particle remains at the top of the larger hill the less the effect of the friction during the motion from the smaller to the larger hill. As $h \to 0$ the particle spends longer and longer at the top of the larger hill and in the limit $h = 0$ the time spent

at the top diverges making the friction force irrelevant. This is as it must be since when the two hills are equal in height we must have no dissapation of energy via friction.

Our analysis tells us three things. First; As the magnetic field gets small and the co-existence curve is approached the order parameter in the interior of the droplet approaches the stable state value. This is the translation back into the $\phi(r)$ language of the statement that the particle starts closer to the top of the larger hill as $h \to 0$. Second; The time spent near the top of the bigger hill diverges as $h \to 0$. This translates into a divergent droplet radius as $h \to 0$. Finally, the interface between the droplet interior and the outside metastable state can be treated separately from the bulk or interior. This is because the interface is the motion from peak to peak in fig. 4.1 and the interior is the motion in the neighborhood of the bigger peak. Clearly this separation is not exact but as the droplet radius diverges in the $h \to 0$ limit is becomes exact. As a consequence the surface profile of the droplet can be approximated extremely well in the $h \to 0$ limit by the solution to

$$-\frac{d^2\phi(r)}{dr^2} - 2|\epsilon|\phi(r) + 4\phi^3(r) = 0 \tag{4.34}$$

where we have set $h = 0$ and neglected the friction force. Equation 4.34 gives an accurate description of the surface profile in the small h limit but contains no information about the droplet size.

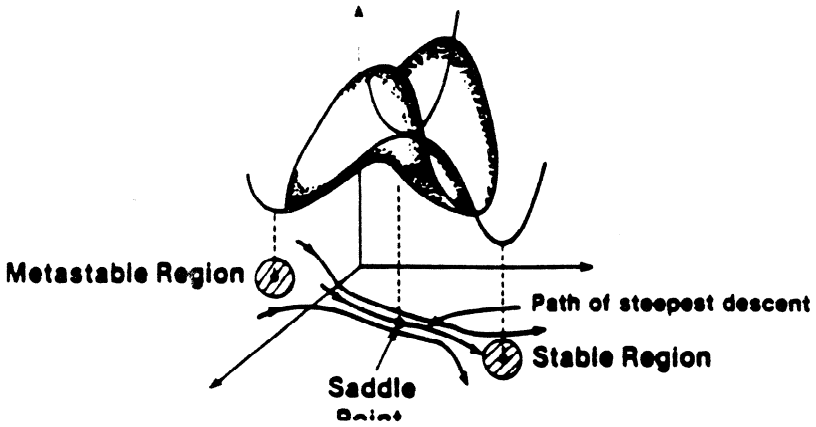

Fig. 4.2 Schematic drawing of a saddle point in function space.

The picture we have put forward is that the system is trapped in a metastable state due to the fact that it is stable to small amplitude fluctuations, which we have been treating within the Gaussian approximation. There are however large amplitude fluctuations which cannot be treated in the Gaussian approximation that allow the system to escape from

the metastable trap. These fluctuations must overcome a barrier which manifests itself mathematically as a saddle point in function space for large βR^d. The meaning of the saddle point is twofold. First, the saddle point droplet is the critical droplet, i. e. the smallest one that makes it. There are larger droplets, droplets larger than the critical size, as well as droplets with different shapes that will also grow and take the system out of the metastable state but these are not given by the solution to eq. 4.9 and in the limit $\beta R^d \to \infty$ are extremely improbable. The second meaning to the saddle point is that there are droplet modes or fluctuations, for example surface deformations, that are orthogonal to the path of steepest descent down from the droplet saddle point. These modes may be important in calculating the metastable state lifetime and we will have to examine them carefully.

It is also important to remember that the nucleation we are considering with these methods is the steady state nucleation described by the Becker-Döring theory discussed in Lesson 3.

The solution to eq. 4.34 which satisfies our boundary conditions is known to be

$$\bar{\phi}(r) = \pm\left[\frac{|\epsilon|}{2}\right]^{1/2} \tanh\left[\sqrt{2}|\epsilon|^{1/2}(r - r_o)\right] \tag{4.35}$$

The quantity r_o is the location of the center of the interface and is arbitrary. This solution satisfies our boundary conditions and is usually referred to as the kink solution or the classical droplet or bubble solution. Note that as $r - r_o \to \pm\infty$ the solution approaches $\pm\sqrt{\epsilon}/\sqrt{2}$ which are the stable and metastable values of the order parameter as $h \to 0$.

Away from the critical point the droplet described by eq. 4.35 is compact, resembles the metastable phase in its interior and has distinct interior and surface. These are precisely the characteristics assumed by the classical theory presented in Lesson 1.

One can use the solution in eq. 4.35 to obtain some information about the dependence of the droplet size as a function of h and about the nucleation rate. We will consider these problems in the next Lesson.

References Lesson 4

1. *Modern Theory of Critical Phenomena*, S. K. Ma, Benjamin (Reading MA, 1976)

2. *Field Theory, the Renormalization Group and Critical Phenomena*, D. Amit, Academic Press (London, 1978)

3. *Theory of Functionals and of Integral and Integro-Differential Equations*, V. Volterra, Dover (New York, 1959)

4. *Techniques and Applications of Path Integration*, L. Schulman, Wiley (New York, 1981)

5. see ref. 11, Lesson 3